Journal Pre-proof

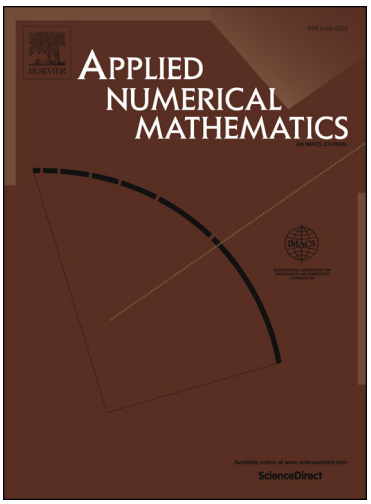

Linear implicit finite difference methods with energy conservation property for space fractional Klein-Gordon-Zakharov system

Jianqiang Xie, Quanxiang Wang and Zhiyue Zhang

PII: S0168-9274(21)00145-8
DOI: https://doi.org/10.1016/j.apnum.2021.05.016
Reference: APNUM 4125

To appear in: *Applied Numerical Mathematics*

Received date: 31 January 2021
Revised date: 18 April 2021
Accepted date: 17 May 2021

Please cite this article as: J. Xie, Q. Wang and Z. Zhang, Linear implicit finite difference methods with energy conservation property for space fractional Klein-Gordon-Zakharov system, *Applied Numerical Mathematics*, doi: https://doi.org/10.1016/j.apnum.2021.05.016.

This is a PDF file of an article that has undergone enhancements after acceptance, such as the addition of a cover page and metadata, and formatting for readability, but it is not yet the definitive version of record. This version will undergo additional copyediting, typesetting and review before it is published in its final form, but we are providing this version to give early visibility of the article. Please note that, during the production process, errors may be discovered which could affect the content, and all legal disclaimers that apply to the journal pertain.

© 2021 Published by Elsevier.

Journal Pre-proof

Highlights

- It is significant to develop unconditionally convergent high-order linearly implicit numerical schemes with preservation properties for solving space fractional Klein-Gordon-Zakharov system.
- New auxiliary equations $\frac{\partial u}{\partial t} = -v$ and $\frac{\partial \phi}{\partial t} = \frac{\partial^2 \psi}{\partial x^2}$ are introduced to transform the original fractional Klein-Gordon-Zakharov system into the corresponding equivalent system of equations exactly.
- We develop and analyze two novel linearly implicit energy conservative difference schemes for the transformed Klein-Gordon-Zakharov system.
- The discrete energy conservation properties, unconditional convergence of the suggested schemes are proved rigidly.
- Numerical examples are performed to investigate the physical behavior of the wave propagation and confirm efficiency of the proposed schemes.

Journal Pre-proof

Journal Pre-proof

Linear implicit finite difference methods with energy conservation property for space fractional Klein-Gordon-Zakharov system

Jianqiang Xie[1], Quanxiang Wang[2], and Zhiyue Zhang[3] *

[1] *School of Mathematical Sciences, Anhui University, Hefei 230601, China*
[2] *College of Science, Nanjing Agricultural University, Nanjing 210031, China*
[3] *School of Mathematical Sciences, Jiangsu Key Laboratory for NSLSCS, Nanjing Normal University, Nanjing 210023, China*

Abstract

In this article, novel linearized implicit difference schemes with energy conservation property for fractional Klein-Gordon-Zakharov system are constructed and analyzed. The important feature of the article is that new auxiliary equations $\frac{\partial u}{\partial t} = -v$ and $\frac{\partial \phi}{\partial t} = \frac{\partial^2 \psi}{\partial x^2}$ are introduced to transform the original fractional Klein-Gordon-Zakharov system into an equivalent system of equations exactly. Especially, two kinds of efficacious difference operators, the leap-frog and modified Crank-Nicolson methods are respectively utilized to establish the linearized implicit difference schemes with energy conservation property for simulating the propagation of transformed equations. And above all, by employing the discrete energy method, we have proven that the constructed difference algorithms enjoy the convergence order of $\mathcal{O}(\Delta t^2 + h^2)$ and $\mathcal{O}(\Delta t^2 + h^4)$ in L^∞- and L^2-norms, without imposing any restrictive conditions on the grid ratio compared with the existing literature. Two numerical examples are carried out to investigate the physical behaviors of the wave propagation and substantiate the effectiveness of the suggested schemes.

Keywords: Fractional Klein-Gordon-Zakharov system; Linear implicit finite difference methods; Energy conservative methods; Unconditional convergence

Mathematics Subject Classification: 65M06, 35R11.

*Corresponding author. E-mail addresses: xiejq1025@163.com (J. Xie), wangquanxiang163@163.com (Q. Wang), zhangzhiyue@njnu.edu.cn (Z. Zhang)

Journal Pre-proof

1 Introduction

The article aims at the numerical approximation to the following nonlinear space fractional Klein-Gordon-Zakharov (KGZ) system, which delineates the interaction of a Langmuir waves and an ion-acoustic waves in plasma,

$$\begin{cases} \dfrac{\partial^2 u}{\partial t^2} + (-\Delta)^{\frac{\gamma}{2}} u + u + u\phi + |u|^2 u = 0, \ \ x \in \mathbb{R}, \ \ 0 < t \leq T, \\ \dfrac{\partial^2 \phi}{\partial t^2} - \dfrac{\partial^2 \phi}{\partial x^2} - \dfrac{\partial^2 |u|^2}{\partial x^2} = 0, \ \ x \in \mathbb{R}, \ \ 0 < t \leq T, \end{cases} \tag{1}$$

subject to the following initial conditions

$$u(x,0) = u_0(x), \quad \frac{\partial u}{\partial t}(x,0) = u_1(x), \quad \phi(x,0) = \phi_0(x), \quad \frac{\partial \phi}{\partial t}(x,0) = \phi_1(x), \ \ x \in \mathbb{R}, \tag{2}$$

and boundary conditions

$$u(x,t) = 0, \quad \phi(x,t) = 0, \quad x \in \mathbb{R}\backslash\Omega, \ \ \Omega = (a,b), \quad t \in [0,T], \tag{3}$$

where $(1 < \gamma \leq 2)$, and $u(x,t)$ stands for the fast time scale component of the electric field produced by electrons, and ϕ denotes the ion density fluctuation from the constant equilibrium. Assume that known smooth functions $u_0(x)$, $u_1(x)$, $\phi_0(x)$ and $\phi_1(x)$ are spatially compactly supported. The fractional Laplacian in (1) can be equivalently represented by the following Riesz fractional derivative [1]

$$-(-\Delta)^{\frac{\gamma}{2}} u(x,t) = \frac{\partial^\gamma u(x,t)}{\partial |x|^\gamma} = -\frac{1}{2\cos(\frac{\pi\gamma}{2})}[{}_{-\infty}D_x^\gamma u(x,t) + {}_xD_\infty^\gamma u(x,t)], \tag{4}$$

where the definition of ${}_{-\infty}D_x^\gamma u(x,t)$ and ${}_xD_\infty^\gamma u(x,t)$ can be found in [2]. Note that as $\gamma = 2$, the system (1)-(3) collapses to the standard KGZ system, which has been investigated by some researchers from the theoretical and numerical perspectives [3–10].

Besides, it has been shown that (1)-(3) owns the following continuous energy conservation law [11]

$$E(t) := \int_{\mathbb{R}} [(\frac{\partial u}{\partial t})^2 + ((-\Delta)^{\gamma/4} u)^2 + u^2 + \frac{1}{2}|u|^4 + \frac{1}{2}(\frac{\partial \varphi}{\partial x})^2 + \frac{1}{2}\phi^2 + |u|^2\phi]\mathrm{d}x \equiv E(0), \ \ t \geq 0, \tag{5}$$

where $(-\Delta)^{\gamma/4} u(x,t) = \mathcal{F}^{-1}(|\xi|^{\gamma/2}\mathcal{F}u(\xi,t))$ (cf. [12]) and the auxiliary variable φ is introduced by $\frac{\partial^2 \varphi}{\partial x^2} = \frac{\partial \phi}{\partial t}$ with $\lim\limits_{|x|\to\infty} \varphi = 0$.

It is well-known that physical property-preserving (including energy, mass, boundedness,etc) numerical methods [13–17, 19–24] are of great importance for simulating nonlinear wave equations because of their good numerical stability and high resolution. As research continues in the theory and analysis of fractional differential equations [25, 26], the study of numerical methods of fractional differential equations draws more attention. Because of the solutions of fractional differential equations involving special functions [2], such as Mittag-Leffler function, Fox-H function, Bernoulli numbers, and so on, it is difficult to obtain the explicit formulations of their analytical

Journal Pre-proof

solutions. It is also worth mentioning that the studies of Bernoulli numbers and functions [27–29] have also been applied to solve the fractional differential equations. Over few decades, some excellent numerical methods including fast algorithms for the space fractional problems have been developed [30–37]. More recently, some (modified) energy conservative numerical methods have been proposed for fractional Schrödinger equation [38–41]. However, only a few efficient physical property-preserving numerical methods are established for simulating the fractional KGZ system. For example, [11] developed an implicit difference algorithm with preservation property for resolving the governing equations. [42] constructed a nonlinear fully implicit difference algorithm for fractional KGZ equations. [43] studied an explicit difference algorithm with energy conservation for the underlying equations. See also references [44–49] for developing nonlinear conservative numerical methods and explicit schemes to explore the nonlinear fractional wave equation. As discussed above, the energy conservative numerical methods mentioned above are almost fully implicit and explicit numerical schemes, which may not be desired for large-scale numerical simulations. As we know, adopting a fully implicit scheme for a nonlinear problem often demands to calculate a nonlinear system of equations at per time step. This seems to be time-consuming compared to linearly implicit methods [16–18]. An explicit scheme may reduce the underlying problem, and will often have the Courant-Friedrichs-Levyor (CFL) restriction condition for the stability analyse. Hence, it is interesting to create efficient numerical schemes with energy conservation to solve KGZ equations in fractional setting in long time simulations.

To our knowledge, there are few efficient and easy-to-implement physical property-preserving numerical methods for solving fractional KGZ system so far. The purpose of the article is to establish the linearized implicit unconditional high-order numerical methods with energy conservation property and attain the corresponding error estimations. In the article, we develop and analyse the new linearized implicit second-order and fourth-order difference schemes with energy conservation property for simulating the space fractional KGZ equations under the homogeneous Dirichlet boundary condition. First, by introducing the auxiliary variables $\frac{\partial u}{\partial t} = -v$ and $\frac{\partial \phi}{\partial t} = \frac{\partial^2 \psi}{\partial x^2}$, we can change the original fractional Klein-Gordon-Zakharov system into the corresponding equivalent four coupled system of equations. Accordingly, two types of efficient difference operators and second-order time-stepping method are respectively adopted to create the linearized implicit finite difference methods with energy conservation for solving the reformulated equations. The energy conservation and theoretical analysis of the underlying algorithms are obtained. It has been validated that the established algorithms enjoy the rate of $\mathcal{O}(\Delta t^2 + h^2)$ and $\mathcal{O}(\Delta t^2 + h^4)$ in L^∞- and L^2-norms, respectively. At last, two examples are carried out to illustrate the effectiveness and the dynamical behaviors of our underlying algorithms.

The structure of the article is laid out as follows. We discuss the establishment of a new linear difference algorithm with energy conservation property for the transformed equations in Section 2. The theoretical analysis of suggested linear difference algorithm is carried out in Section 3. Section 4 is aimed at designing a fourth-order linear finite difference scheme with energy conservation property to solve the transformed equations. Two representative examples are carried out to validate the effectiveness of the suggested schemes in Section 5. In Section 6, some conclusions are concluded. Throughout this paper, we utilize the standard notations for

Journal Pre-proof

Sobolev spaces, and employ C to represent a generic positive constant that can select various values in different occasions, and not rely on the mesh sizes h and Δt.

2 A second-order linear finite difference scheme with energy conservation property

In this section, we first supply some notations and lemmas. Afterwards, a new second-order linearized difference scheme with energy conservation property is derived for the reformulated KGZ system (1)–(3). Subsequently, discrete energy conservation law of the underlying algorithm is achieved.

2.1 Notations and lemmas

Taking M, N ($\in \mathbb{Z}^+$), and denote $h=(b-a)/M$ and $\Delta t=T/N$ by the space mesh size and time step size, respectively. Denote by $x_i=a+ih$, $t_k=k\Delta t$, the computational domain $\Omega\times[0,T]$ is covered by $\Omega_h\times\Omega_{\Delta t}$, where $\Omega_h=\{x_i|0\le i\le M\}$ and $\Omega_{\Delta t}=\{t_k|0\le k\le N\}$. Assume the grid function $\{v_i^k|0\le i\le M, 0\le k\le N\}$ is defined on $\Omega_{h\Delta t}$. Accordingly, we present some notations and lemmas.

$\delta_t v_i^{k+1/2}=(v_i^{k+1}-v_i^k)/\Delta t$, $v_i^{k+1/2}=(v_i^{k+1}+v_i^k)/2$, $\mu_t v_i^k=(v_i^{k+1}+v_i^{k-1})/2$, $\mathcal{D}_t v_i^k=(v_i^{k+1}-v_i^{k-1})/(2\Delta t)$, $\delta_t^2 v_i^k=\frac{1}{\Delta t^2}(v_i^{k+1}-2v_i^k+v_i^{k-1})$, $\delta_x v_{i+1/2}^k=(v_{i+1}^k-v_i^k)/h$,

$$
\begin{aligned}
&{}_L\delta_x^\gamma v_i^k=\frac{1}{h^\gamma}\sum_{m=0}^{i+1}w_m^{(\gamma)}v_{i-m+1}^k,\qquad {}_R\delta_x^\gamma v_i^k=\frac{1}{h^\gamma}\sum_{m=0}^{M-i+1}w_m^{(\gamma)}v_{i+m-1}^k,\\
&\delta_x^\gamma v_i^k=\frac{1}{2\cos\frac{\gamma\pi}{2}}({}_L\delta_x^\gamma v_i^k+{}_R\delta_x^\gamma v_i^k),\qquad \delta_x^2 v_i^k=(v_{i+1}^k-2v_i^k+v_{i-1}^k)/h^2,
\end{aligned}
$$

where

$$
\begin{aligned}
&g_0^{(\gamma)}=1,\quad g_{m+1}^{(\gamma)}=(1-\tfrac{\gamma+1}{m+1})g_m^{(\gamma)},\quad m\ge 1,\quad w_0^{(\gamma)}=\lambda_1 g_0^{(\gamma)},\\
&\lambda_1=\frac{\gamma^2+3\gamma+2}{12},\quad \lambda_0=\frac{4-\gamma^2}{6},\quad \lambda_{-1}=\frac{\gamma^2-3\gamma+2}{12},\\
&w_1^{(\gamma)}=\lambda_1 g_1^{(\gamma)}+\lambda_0 g_0^{(\gamma)},\quad w_m^{(\gamma)}=\lambda_1 g_m^{(\gamma)}+\lambda_0 g_{m-1}^{(\gamma)}+\lambda_{-1}g_{m-2}^{(\gamma)},\quad m\ge 2.
\end{aligned}
\tag{6}
$$

Define grid function spaces $V_h=\{v|v=(v_0,v_1,\dots,v_M), v_0=v_M=0\}\subseteq\mathbb{C}^{M+1}$ and $W_h=\{w|w=(w_0,w_1,\dots,w_M), w_0=w_M=0\}\subseteq\mathbb{R}^{M+1}$ on Ω_h. For any $v,w\in V_h$, the discrete inner products and associated norms can be represented as

$$
(v,w)_{l_2}=h\sum_{i=1}^{M-1}v_i\bar{w}_i,\qquad \|v\|_p^p=h\sum_{i=1}^{M-1}|v_i|^p, 1\le p<+\infty,\qquad \|v\|_\infty=\max_{0\le i\le M}|v_i|,
$$

$$
(\delta_x v,\delta_x w)_{l_2}=h\sum_{i=0}^{M-1}(\delta_x v_{i+1/2})(\delta_x w_{i+1/2}),\qquad \|\delta_x v\|_{l_2}^2=(\delta_x v,\delta_x v)_{l_2}.
$$

For simplicity, we write $\|\cdot\|:=\|\cdot\|_{l_2}$.

Journal Pre-proof

Provided that the constant $0 \leq \sigma \leq 1$, the fractional Sobolev norm $\|\cdot\|_{H^\sigma}$ and semi-norm $|\cdot|_{H^\sigma}$ are introduced as

$$\|u\|_{H^\sigma}^2 = \int_{-\pi/h}^{\pi/h} (1+|\xi|^{2\sigma})|\hat{u}(\xi)|^2 d\xi, \quad |u|_{H^\sigma}^2 = \int_{-\pi/h}^{\pi/h} |\xi|^{2\sigma}|\hat{u}(\xi)|^2 d\xi.$$

It is easy to find that $\|u\|_{H^0}^2 = \|u\|^2$ and $\|u\|_{H^\sigma}^2 = \|u\|^2 + |u|_{H^\sigma}^2$.

Lemma 1 (cf. [50]) Suppose that $u \in L^1(\mathbb{R})$ and

$$u \in \mathcal{C}^{2+\gamma}(\mathbb{R}) := \left\{ u \Big| \int_{-\infty}^{\infty} (1+|\xi|)^{2+\gamma} |\hat{u}(\xi)| d\xi < \infty \right\},$$

then for given h, we arrive at

$${}_{-\infty}D_x^\gamma u(x) = {}_L\delta_x^\gamma u(x) + \mathcal{O}(h^2), \quad {}_xD_{+\infty}^\gamma u(x) = {}_R\delta_x^\gamma u(x) + \mathcal{O}(h^2).$$

Lemma 2 (cf. [38]) There exists a unique linear operator $\Lambda^\gamma : V_h \to V_h$, such that $(\delta_x^\gamma u, v) = (\Lambda^\gamma u, \Lambda^\gamma v)$ for $\forall u, v \in V_h$.

Lemma 3 (cf. [38, 50]) For $1 < \gamma \leq 2$ and $u \in V_h$, we derive $C_\gamma |u|_{H^{\frac{\gamma}{2}}}^2 \leq (\delta_x^\gamma u, u) \leq |u|_{H^{\frac{\gamma}{2}}}^2$, where $C_\gamma = \frac{2^\gamma(1-\gamma^2)}{3\pi^\gamma \cos\frac{\gamma\pi}{2}} > 0$.

Lemma 4 (cf. [38]) For $\frac{1}{2} < \sigma \leq 1$, there exists a positive constant $C_\sigma = C(\sigma)$ independent of $h > 0$ such that $\|u\|_\infty \leq C_\sigma \|u\|_{H^\sigma}$.

2.2 Construction of a second-order linear energy conservative difference scheme

This subsection is devoted to the establishment of the new second-order linear difference scheme with energy conservation property for the fractional KGZ system (1)–(3).

To this end, by introducing the auxiliary variables $\frac{\partial u}{\partial t} = -v$ and $\frac{\partial \phi}{\partial t} = \frac{\partial^2 \psi}{\partial x^2}$, then we can reformulate the space fractional KGZ system (1)–(3) as the equivalent system of equations

$$\frac{\partial u}{\partial t} = -v, \tag{7}$$

$$\frac{\partial v}{\partial t} = (-\Delta)^{\frac{\gamma}{2}} u + u + u\phi + |u|^2 u, \tag{8}$$

$$\frac{\partial \phi}{\partial t} = \frac{\partial^2 \psi}{\partial x^2}, \tag{9}$$

$$\frac{\partial \psi}{\partial t} = \phi + |u|^2, \tag{10}$$

endowed with the associated initial conditions

$$u(x,0) = u_0(x), \quad v(x,0) = v_0(x), \quad \phi(x,0) = \phi_0(x), \quad \psi(x,0) = \psi_0(x), \ \ x \in \mathbb{R}, \tag{11}$$

and boundary conditions

$$u(x,t) = 0, \ \ v(x,t) = 0, \ \ \phi(x,t) = 0, \ \ \psi(x,t) = 0, \ \ x \in \mathbb{R}\backslash\Omega, \ \ \Omega = (a,b), \quad t \in [0,T]. \tag{12}$$

Journal Pre-proof

Here, $\psi(x,0)$ is determined by the problem as

$$\begin{aligned} &\frac{\partial^2\psi}{\partial x^2}(x,0)=\frac{\partial\phi}{\partial t}(x,0)=\phi_1(x),\\ &\psi(x,0)=0, \quad x\in\mathbb{R}\backslash\Omega. \end{aligned} \tag{13}$$

Obviously, the analytical expression of (13) is available.

It is worth pointing out that, performing the both sides of (7)–(10) with $\frac{\partial v}{\partial t}$, $\frac{\partial u}{\partial t}$, $\frac{\partial \psi}{\partial t}$, $\frac{\partial \phi}{\partial t}$ respectively, integrating over Ω, by collecting and regrouping the resulting formulae, we can derive that the reformulated system (7)–(13) preserves the following total energy

$$\widetilde{E}(t):=\int_{\mathbb{R}}[v^2+((-\Delta)^{\gamma/4}u)^2+u^2+\frac{1}{2}|u|^4+\frac{1}{2}(\frac{\partial\psi}{\partial x})^2+\frac{1}{2}\phi^2+|u|^2\phi]\mathrm{d}x\equiv\widetilde{E}(0),\ \ t\geq 0. \tag{14}$$

Therefore, it is meaningful to construct the efficient numerical schemes with discrete energy preservation.

Remark 1 From the energy conservation (14), combined with ε-inequality $\int_{\mathbb{R}}|u|^2\phi\mathrm{d}x\leq\frac{\varepsilon}{4}\|\phi\|_{L^2}^2+\varepsilon\|u\|_{L^4}^4$, and fractional Gagliardo-Nirenberg inequality $\int_{\mathbb{R}}|u|^4\mathrm{d}x\leq C(\int_{\mathbb{R}}|(-\Delta)^{\gamma/4}u|^2\mathrm{d}x)^{\frac{2}{\gamma}}\cdot(\int_{\mathbb{R}}|u|^2\mathrm{d}x)^{4-\frac{2}{\gamma}}$, we can obtain

$$\|v\|_{L^2}^2+\|(-\Delta)^{\gamma/4}u\|_{L^2}^2+\|u\|_{L^2}^2+\|\frac{\partial\psi}{\partial x}\|_{L^2}^2+\|\phi\|_{L^2}^2\leq C.$$

In what follows, we shall discuss the establishment of the new second-order linearized scheme for the transformed system (7)–(13).

Assume that U_i^k, V_i^k, Φ_i^k and Ψ_i^k are the numerical approximations to $u(x_i,t_k)$, $v(x_i,t_k)$, $\phi(x_i,t_k)$ and $\psi(x_i,t_k)$, respectively. The grid functions can be defined as $u_i^k=u(x_i,t_k)$, $v_i^k=v(x_i,t_k)$, $\phi_i^k=\phi(x_i,t_k)$, $\psi_i^k=\psi(x_i,t_k)$, $0\leq i\leq M$, $0\leq k\leq N$.

Considering (7)–(10) at the point (x_i,t_k) yields

$$\frac{\partial u}{\partial t}(x_i,t_k)=-v(x_i,t_k), \tag{15}$$

$$\frac{\partial v}{\partial t}(x_i,t_k)=(-\Delta)^{\frac{\gamma}{2}}u(x_i,t_k)+u(x_i,t_k)+u(x_i,t_k)\phi(x_i,t_k)+|u(x_i,t_k)|^2u(x_i,t_k), \tag{16}$$

$$\frac{\partial\phi}{\partial t}(x_i,t_k)=\frac{\partial^2\psi}{\partial x^2}(x_i,t_k), \tag{17}$$

$$\frac{\partial\psi}{\partial t}(x_i,t_k)=\phi(x_i,t_k)+|u(x_i,t_k)|^2. \tag{18}$$

By using second-order central difference scheme, Lemma 1 and leap-frog scheme for approaching the obtained equations (15)–(18) in space and time directions, respectively, we derive the difference scheme as follows

$$\mathcal{D}_tU_i^k=-\mu_tV_i^k, \tag{19}$$

$$\mathcal{D}_tV_i^k=\delta_x^\gamma\mu_tU_i^k+\mu_tU_i^k+\mu_tU_i^k\Phi_i^k+|U_i^k|^2\mu_tU_i^k, \tag{20}$$

$$\mathcal{D}_t\Phi_i^k=\delta_x^2\mu_t\Psi_i^k, \tag{21}$$

Journal Pre-proof

$$\mathcal{D}_t\Psi_i^k = \mu_t\Phi_i^k + |U_i^k|^2. \tag{22}$$

Observe that the three-level scheme above still demand U_i^1, V_i^1, Φ_i^1 and Ψ_i^1 to initialize the computation. Here, we adopt the following modified Crank-Nicolson second-order difference scheme

$$\delta_t U_i^{\frac{1}{2}} = -V_i^{\frac{1}{2}}, \tag{23}$$

$$\delta_t V_i^{\frac{1}{2}} = \delta_x^\gamma U_i^{\frac{1}{2}} + U_i^{\frac{1}{2}} + U_i^{\frac{1}{2}}\Phi_i^{(\frac{1}{2})} + |U_i^{(\frac{1}{2})}|^2 U_i^{\frac{1}{2}}, \tag{24}$$

$$\delta_t \Phi_i^{\frac{1}{2}} = \delta_x^2 \Psi_i^{\frac{1}{2}}, \tag{25}$$

$$\delta_t \Psi_i^{\frac{1}{2}} = \Phi_i^{\frac{1}{2}} + |U_i^{(\frac{1}{2})}|^2, \tag{26}$$

where $U^{(\frac{1}{2})}$ and $\Phi^{(\frac{1}{2})}$ are computed by the following scheme

$$U_i^{(\frac{1}{2})} = u(x_i, 0) + \frac{\Delta t}{2}\frac{\partial u}{\partial t}(x_i, 0), \tag{27}$$

$$\Phi_i^{(\frac{1}{2})} = \phi(x_i, 0) + \frac{\Delta t}{2}\frac{\partial \phi}{\partial t}(x_i, 0). \tag{28}$$

And the related initial and boundary conditions are provided as follows:

$$U_i^0 = u_0(x_i),\ \ V_i^0 = v_0(x_i),\ \ \Phi_i^0 = \phi_0(x_i),\ \ \Psi_i^0 = \tilde{\Psi}_i^0, \tag{29}$$

$$U_0^k = U_M^k = 0,\ \ V_0^k = V_M^k = 0,\ \ \Phi_0^k = \Phi_M^k = 0,\ \ \Psi_0^k = \Psi_M^k = 0, \tag{30}$$

where Ψ_i^0 is calculated by the following scheme

$$\begin{aligned} &\delta_x^2 \Psi_i^0 = \phi_1(x_i),\ \ 1 \le i \le M-1, \\ &\Psi_0^0 = \Psi_M^0 = 0. \end{aligned} \tag{31}$$

2.3 Discrete energy conservation property I

This subsection is devoted to the discrete energy conservation property I of the suggested scheme (19)–(31).

Theorem 1 Suppose that U_i^k, V_i^k, Φ_i^k and Ψ_i^k are the numerical solutions of the suggested difference algorithm (19)–(31). Then the scheme (19)–(31) admits the energy preservation property, i.e.,

$$E^k = E^0, \tag{32}$$

where

$$\begin{aligned} E^k = &(\|V^{k+1}\|^2 + \|V^k\|^2) + (\|\Lambda^\gamma U^{k+1}\|^2 + \|\Lambda^\gamma U^k\|^2) + (\|U^{k+1}\|^2 + \|U^k\|^2) \\ &+\frac{1}{2}(\|\delta_x \Psi^{k+1}\|^2 + \|\delta_x \Psi^k\|^2) + \frac{1}{2}(\|\Phi^{k+1}\|^2 + \|\Phi^k\|^2) \\ &+ \sum_{i=1}^{M-1} |U_i^k|^2 |U_i^{k+1}|^2 h + \sum_{i=1}^{M-1} [|U_i^{k+1}|^2 \Phi_i^k + |U_i^k|^2 \Phi_i^{k+1}] h \end{aligned}$$

Journal Pre-proof

is the discrete energy.

Proof. Multiplying the inner product of (19) with $\mathcal{D}_t V^k$, acting the inner product of (20) with $\mathcal{D}_t U^k$, with the aid of Lemma 2, we deduce

$$\begin{aligned}&(\|V^{k+1}\|^2-\|V^{k-1}\|^2)+(\|\Lambda^\gamma U^{k+1}\|^2-\|\Lambda^\gamma U^{k-1}\|^2)+(\|U^{k+1}\|^2-\|U^{k-1}\|^2)\\&+\sum_{i=1}^{M-1}[(U_i^{k+1})^2-(U_i^{k-1})^2]\Phi_i^k h+\sum_{i=1}^{M-1}|U_i^k|^2[|U_i^{k+1}|^2-|U_i^{k-1}|^2]h=0.\end{aligned}\tag{33}$$

Performing the inner product of (21) with $\mathcal{D}_t\Psi^k$, testing the inner product between (22) and $\mathcal{D}_t\Phi^k$, and using the discrete Green formula, then adding the resulting formulae, we obtain

$$\frac{1}{2}(\|\delta_x\Psi^{k+1}\|^2-\|\delta_x\Psi^{k-1}\|^2)+\frac{1}{2}(\|\Phi^{k+1}\|^2-\|\Phi^{k-1}\|^2)+\sum_{i=1}^{M-1}|U_i^k|^2(\Phi_i^{k+1}-\Phi_i^{k-1})h=0.\tag{34}$$

Combining (33) and (34), collecting and regrouping the resulting terms, we further derive the claimed result. The proof is completed. □

3 Error estimations of the proposed second-order difference scheme

This section is devoted to investigating the error estimations of (19)–(26). To do so, superseding U_i^k, V_i^k, Φ_i^k and Ψ_i^k in (19)–(26) with the corresponding analytical solutions u_i^k, v_i^k, ϕ_i^k and ψ_i^k, afterwards we get the following equations

$$\mathcal{D}_t u_i^k=-\mu_t v_i^k+R_{1i}^k,\tag{35}$$

$$\mathcal{D}_t v_i^k=\delta_x^\gamma\mu_t u_i^k+\mu_t u_i^k+\mu_t u_i^k\phi_i^k+|u_i^k|^2\mu_t u_i^k+R_{2i}^k,\tag{36}$$

$$\mathcal{D}_t \phi_i^k=\delta_x^2\mu_t\psi_i^k+R_{3i}^k,\tag{37}$$

$$\mathcal{D}_t \psi_i^k=\mu_t\phi_i^k+|u_i^k|^2+R_{4i}^k,\tag{38}$$

$$\delta_t u_i^{\frac{1}{2}}=-v_i^{\frac{1}{2}}+R_{5i}^{\frac{1}{2}},\tag{39}$$

$$\delta_t v_i^{\frac{1}{2}}=\delta_x^\gamma u_i^{\frac{1}{2}}+u_i^{\frac{1}{2}}+u_i^{\frac{1}{2}}\phi_i^{(\frac{1}{2})}+|u_i^{(\frac{1}{2})}|^2u_i^{\frac{1}{2}}+R_{6i}^{\frac{1}{2}},\tag{40}$$

$$\delta_t \phi_i^{\frac{1}{2}}=\delta_x^2\psi_i^{\frac{1}{2}}+R_{7i}^{\frac{1}{2}},\tag{41}$$

$$\delta_t \psi_i^{\frac{1}{2}}=\phi_i^{\frac{1}{2}}+|u_i^{(\frac{1}{2})}|^2+R_{8i}^{\frac{1}{2}}.\tag{42}$$

Using Taylor expansions and after a few calculations, we can obtain the following lemma 5.

Lemma 5 Suppose that $u(x,t)$, $v(x,t)$, $\phi(x,t)$ and $\psi(x,t)$ are the exact solutions of the equations (7)–(10). Then we arrive at

$$\begin{aligned}&\max_{0\le k\le N}\{\|R_1^k\|,\|R_4^k\|\}\le C\Delta t^2,\ \max_{0\le k\le N}\{\|R_2^k\|,\|R_3^k\|\}\le C(\Delta t^2+h^2),\\&\max_{0\le k\le N}\{\|\mathcal{D}_t R_1^k\|,\|\mathcal{D}_t R_4^k\|\}\le C\Delta t^2,\ \max_{0\le k\le N}\{\|\mathcal{D}_t R_2^k\|,\|\mathcal{D}_t R_3^k\|\}\le C(\Delta t^2+h^2),\\&\max\{\|R_5^{\frac{1}{2}}\|,\|R_8^{\frac{1}{2}}\|\}\le C\Delta t^2,\ \max\{\|R_6^{\frac{1}{2}}\|,\|R_7^{\frac{1}{2}}\|\}\le C(\Delta t^2+h^2).\end{aligned}$$

Journal Pre-proof

For the sake of notations, we define the error functions e_i^k, η_i^k, ξ_i^k and θ_i^k as follows

$$e_i^k = u_i^k - U_i^k,\ \ \eta_i^k = v_i^k - V_i^k,\ \ \xi_i^k = \phi_i^k - \Phi_i^k,\ \ \theta_i^k = \psi_i^k - \Psi_i^k,\ \ 0 \le i \le M,\ \ 0 \le k \le N.$$

Subsequently, subtracting (19)–(26) from (35)–(42), and combining the initial and boundary conditions, we get the error equations as follows:

$$\mathcal{D}_t e_i^k = -\mu_t \eta_i^k + R_{1i}^k, \tag{43}$$

$$\mathcal{D}_t \eta_i^k = \delta_x^\gamma \mu_t e_i^k + \mu_t e_i^k + \mu_t u_i^k \phi_i^k - \mu_t U_i^k \Phi_i^k + |u_i^k|^2 \mu_t u_i^k - |U_i^k|^2 \mu_t U_i^k + R_{2i}^k, \tag{44}$$

$$\mathcal{D}_t \xi_i^k = \delta_x^2 \mu_t \theta_i^k + R_{3i}^k, \tag{45}$$

$$\mathcal{D}_t \theta_i^k = \mu_t \xi_i^k + |u_i^k|^2 - |U_i^k|^2 + R_{4i}^k, \tag{46}$$

$$\delta_t e_i^{\frac{1}{2}} = -\eta_i^{\frac{1}{2}} + R_{5i}^{\frac{1}{2}}, \tag{47}$$

$$\delta_t \eta_i^{\frac{1}{2}} = \delta_x^\gamma e_i^{\frac{1}{2}} + e_i^{\frac{1}{2}} + e_i^{\frac{1}{2}} \phi_i^{(\frac{1}{2})} + |u_i^{(\frac{1}{2})}|^2 e_i^{\frac{1}{2}} + R_{6i}^{\frac{1}{2}}, \tag{48}$$

$$\delta_t \xi_i^{\frac{1}{2}} = \delta_x^2 \theta_i^{\frac{1}{2}} + R_{7i}^{\frac{1}{2}}, \tag{49}$$

$$\delta_t \theta_i^{\frac{1}{2}} = \xi_i^{\frac{1}{2}} + R_{8i}^{\frac{1}{2}}, \tag{50}$$

$$e_i^0 = 0,\ \ \eta_i^0 = 0,\ \ \xi_i^0 = 0,\ \ \theta_i^0 = \Psi_0(x_i) - \tilde{\Psi}_i^0, \tag{51}$$

$$e_0^k = e_M^k = 0,\ \ \eta_0^k = \eta_M^k = 0,\ \ \xi_0^k = \xi_M^k = 0,\ \ \theta_0^k = \theta_M^k = 0. \tag{52}$$

By using (13) and (31), remark that the following fact holds:

$$\|\delta_x \theta^0\| \le C h^2. \tag{53}$$

Theorem 2 Assume that $u(x,t)$, $v(x,t)$, $\phi(x,t)$ and $\psi(x,t)$ are the exact solutions of (7)–(10). Let U_i^k, V_i^k, Φ_i^k and Ψ_i^k be the associated numerical solutions of the suggested algorithm (19)–(26). Provided that the condition of Lemma 5 is valid, then as Δt and h are small enough, we conclude the following optimal error estimates for the scheme (19)–(26)

$$\begin{aligned} &\|e^k\|_\infty \le C(\Delta t^2 + h^2),\ \ \|U^k\|_\infty \le M_1 + 1, \\ &\max_{0\le k\le N}\{\|e^k\|, \|\eta^k\|, \|\xi^k\|, \|\delta_x \theta^k\|\} \le C(\Delta t^2 + h^2), \end{aligned} \tag{54}$$

where $M_1 = \max\limits_{0\le t\le T} \|u(\cdot,t)\|_\infty$.

Proof. Multiplying the inner product of (47) with $\delta_t e^{\frac{1}{2}}$, and performing the inner product of (48) with $\delta_t e^{\frac{1}{2}}$, by Lemma 2, we obtain

$$\begin{aligned} &(\|\eta^1\|^2 - \|\eta^0\|^2) + (\|\Lambda^\gamma e^1\|^2 - \|\Lambda e^0\|^2) + (\|e^1\|^2 - \|e^0\|^2) + \sum_{i=1}^{M-1} \phi_i^{(\frac{1}{2})}[(e_i^1)^2 - (e_i^0)^2]h \\ &+ \sum_{i=1}^{M-1} |u_i^{(\frac{1}{2})}|^2[(e_i^1)^2 - (e_i^0)^2]h = 2\Delta t(R_5^{\frac{1}{2}}, \delta_t \eta^{\frac{1}{2}}) - 2\Delta t(R_6^{\frac{1}{2}}, \delta_t e^{\frac{1}{2}}). \end{aligned} \tag{55}$$

Journal Pre-proof

Multiplying the inner product of (49) with $\delta_t\theta^{\frac{1}{2}}$, and performing the inner product of (50) with $\delta_t\xi^{\frac{1}{2}}$, by discrete Green formula, we have

$$(\|\delta_x\theta^1\|^2-\|\delta_x\theta^0\|^2)+(\|\xi^1\|^2-\|\xi^0\|^2)=2\Delta t(R_7^{\frac{1}{2}},\delta_t\theta^{\frac{1}{2}})-2\Delta t(R_8^{\frac{1}{2}},\delta_t\xi^{\frac{1}{2}}). \tag{56}$$

By virtue of (27)–(28), (51), (53), it is readily to check that the following formulae hold:

$$\begin{aligned}&\|e^0\|=0,\ \ \|\eta^0\|=0,\ \ \|\Lambda^\gamma\eta^0\|=0,\ \ \|\xi^0\|=0,\\&\|\delta_x\theta^0\|\le Ch^2,\ \ |\phi_i^{(\frac{1}{2})}|\le C,\ \ |u_i^{(\frac{1}{2})}|^2\le C.\end{aligned} \tag{57}$$

Combining (55) and (56), using (57), ε-inequality and poincáre inequality [51], we can deduce that

$$\|\eta^1\|^2+\|\Lambda^\gamma e^1\|^2+\|e^1\|^2+\|\delta_x\theta^1\|^2+\|\xi^1\|^2\le C(\Delta t^2+h^2)^2, \tag{58}$$

which further implies that

$$\max\{\|\eta^1\|,\|e^1\|,\|\xi^1\|,\|\delta_x\theta^1\|\}\le C(\Delta t^2+h^2),\ \ \|e^1\|_\infty\le C(\Delta t^2+h^2), \tag{59}$$

where Lemma 3 and Lemma 4 are invoked to (59).

In what follows, we shall prove the claimed results are valid for $2\le k\le N$.

As the priori bounds of scheme (19)–(22) can not be derived directly. Here, we shall utilize the "cut-off" function technique [52] to discuss the convergence analysis of (19)–(22).

Selecting a smooth function $f(s)\in C^\infty(\mathbb{R}^+)$ such that $f(s)=1$ as $0\le s\le 1$, $f(s)=0$ as $s\ge 2$, and $0\le f(s)\le 1$ for $1\le s\le 2$. Taking a positive number $B=(M_1+1)^2$, and for $s\ge 0$, y_1, $y_2\in\mathbb{R}$, define

$$f_B(s)=sf(s/B),\qquad g(y_1,y_2)=\frac{y_1+y_2}{2}\int_0^1 f_B'(sy_1^2+(1-s)y_2^2)ds.$$

Then, $f_B(s)$ is global Lipschitz satisfying

$$|f_B(s_1)-f_B(s_2)|\le\sqrt{C_B}|\sqrt{s_1}-\sqrt{s_2}|,\qquad\forall s_1,s_2\ge 0, \tag{60}$$

provided that $C_B>0$.

Taking $\widetilde{U}_i^0=U_i^0$, $\widetilde{V}_i^0=V_i^0$, $\widetilde{\Phi}_i^0=\Phi_i^0$, $\widetilde{\Psi}_i^0=\Psi_i^0$, $\widetilde{U}_i^1=U_i^1$, $\widetilde{V}_i^1=V_i^1$, $\widetilde{\Phi}_i^1=\Phi_i^1$, $\widetilde{\Psi}_i^1=\Psi_i^1$, and calculating $\widetilde{U}_i^k$, $\widetilde{V}_i^k$, $\widetilde{\Phi}_i^k$, $\widetilde{\Psi}_i^k$ by

$$\mathcal{D}_t\widetilde{U}_i^k=-\mu_t\widetilde{V}_i^k, \tag{61}$$

$$\mathcal{D}_t\widetilde{V}_i^k=\delta_x^\gamma\mu_t\widetilde{U}_i^k+\mu_t\widetilde{U}_i^k+g(\widetilde{U}_i^{k+1},\widetilde{U}_i^{k-1})\widetilde{\Phi}_i^k+f_B(|\widetilde{U}_i^k|^2)\mu_t\widetilde{U}_i^k, \tag{62}$$

$$\mathcal{D}_t\widetilde{\Phi}_i^k=\delta_x^2\mu_t\widetilde{\Psi}_i^k, \tag{63}$$

$$\mathcal{D}_t\widetilde{\Psi}_i^k=\mu_t\widetilde{\Phi}_i^k+f_B(|\widetilde{U}_i^k|^2). \tag{64}$$

Here $\widetilde{U}_i^k$, $\widetilde{V}_i^k$, $\widetilde{\Phi}_i^k$ and $\widetilde{\Psi}_i^k$ can be referred to as other numerical discretization of $u(x_i,t_k)$, $v(x_i,t_k)$, $\phi(x_i,t_k)$ and $\psi(x_i,t_k)$. Thanks to $f_B(|u^k|^2)=|u^k|^2$ and $g(u^{k+1},u^{k-1})=\frac{u^{k+1}+u^{k-1}}{2}$, we can

Journal Pre-proof

obtain that the local truncation errors of (61)–(64) are same as R_1^k, R_2^k, R_3^k and R_4^k determined by (35)–(38).

The "error" functions $\widetilde{e}_i^k$, $\widetilde{\eta}_i^k$, $\widetilde{\xi}_i^k$ and $\widetilde{\theta}_i^k$ can be denoted as follows:

$$\widetilde{e}_i^k = u_i^k - \widetilde{U}_i^k,\ \ \widetilde{\eta}_i^k = v_i^k - \widetilde{V}_i^k,\ \ \widetilde{\xi}_i^k = \phi_i^k - \widetilde{\Phi}_i^k,\ \ \widetilde{\theta}_i^k = \psi_i^k - \widetilde{\Psi}_i^k,\ \ 0 \le i \le M,\ \ 1 \le k \le N.$$

Then we have the following corresponding error equations

$$\mathcal{D}_t \widetilde{e}_i^k = -\mu_t \widetilde{\eta}_i^k + {R_1}_i^k, \tag{65}$$

$$\begin{aligned}\mathcal{D}_t \widetilde{\eta}_i^k &= \delta_x^\gamma \mu_t \widetilde{e}_i^k + \mu_t \widetilde{e}_i^k + g(u_i^{k+1}, u_i^{k-1})\phi_i^k - g(\widetilde{U}_i^{k+1}, \widetilde{U}_i^{k-1})\widetilde{\Phi}_i^k \\ &\quad + f_B(|u_i^k|^2)\mu_t u_i^k - f_B(|\widetilde{U}_i^k|^2)\mu_t \widetilde{U}_i^k + {R_2}_i^k,\end{aligned} \tag{66}$$

$$\mathcal{D}_t \widetilde{\xi}_i^k = \delta_x^2 \mu_t \widetilde{\theta}_i^k + {R_3}_i^k, \tag{67}$$

$$\mathcal{D}_t \widetilde{\theta}_i^k = \mu_t \widetilde{\xi}_i^k + f_B(|u_i^k|^2) - f_B(|\widetilde{U}_i^k|^2) + {R_4}_i^k. \tag{68}$$

Multiplying the inner product of (65) with $\mathcal{D}_t \eta^k$, and performing the inner product of (66) with $\mathcal{D}_t e^k$, using Lemma 2 and regrouping the resulting formulae, we have

$$\begin{aligned}&2(\|\widetilde{\eta}^{k+1}\|^2 - \|\widetilde{\eta}^{k-1}\|^2) + 4C_B(\|\Lambda^\gamma \widetilde{e}^{k+1}\|^2 - \|\Lambda^\gamma \widetilde{e}^{k-1}\|^2) + 4C_B(\|\widetilde{e}^{k+1}\|^2 - \|\widetilde{e}^{k-1}\|^2) \\ &= 8\Delta t(R_1^k, \mathcal{D}_t \widetilde{\eta}^k) - 16C_B\Delta t(R_2^k, \mathcal{D}_t \widetilde{e}^k) - 16C_B\Delta t(f_B(|u^k|^2)\mu_t u^k - f_B(|\widetilde{U}^k|^2)\mu_t \widetilde{U}^k, \mathcal{D}_t \widetilde{e}^k) \\ &\quad -16C_B\Delta t(g(u^{k+1}, u^{k-1})\phi^k - g(\widetilde{U}^{k+1}, \widetilde{U}^{k-1})\widetilde{\Phi}^k, \mathcal{D}_t \widetilde{e}^k).\end{aligned} \tag{69}$$

Acting the inner product of (67) with $\mathcal{D}_t \theta^k$, and testing the inner product of (68) with $\mathcal{D}_t \xi^k$, using the discrete Green formula, we obtain

$$\begin{aligned}&(\|\widetilde{\xi}^{k+1}\|^2 - \|\widetilde{\xi}^{k-1}\|^2) + (\|\delta_x \widetilde{\theta}^{k+1}\|^2 - \|\delta_x \widetilde{\theta}^{k-1}\|^2) \\ &= 4\Delta t(R_3^k, \mathcal{D}_t \widetilde{\theta}^k) - 4\Delta t(R_4^k, \mathcal{D}_t \widetilde{\xi}^k) - 4\Delta t(f_B(|u^k|^2) - f_B(|\widetilde{U}^k|^2), \mathcal{D}_t \widetilde{\xi}^k).\end{aligned} \tag{70}$$

Noticing that

$$\begin{aligned}&g(u_i^{k+1}, u_i^{k-1})\phi_i^k - g(\widetilde{U}_i^{k+1}, \widetilde{U}_i^{k-1})\widetilde{\Phi}_i^k \\ &= g(u_i^{k+1}, u_i^{k-1})\phi_i^k - g(\widetilde{U}_i^{k+1}, \widetilde{U}_i^{k-1})\phi_i^k + g(\widetilde{U}_i^{k+1}, \widetilde{U}_i^{k-1})\phi_i^k - g(\widetilde{U}_i^{k+1}, \widetilde{U}_i^{k-1})\widetilde{\Phi}_i^k \\ &= [g(u_i^{k+1}, u_i^{k-1}) - g(\widetilde{U}_i^{k+1}, \widetilde{U}_i^{k-1})]\phi_i^k + g(\widetilde{U}_i^{k+1}, \widetilde{U}_i^{k-1})\widetilde{\xi}_i^k.\end{aligned} \tag{71}$$

An application of the definition of $g(x, y)$, after careful calculations, we have

$$|g(\widetilde{U}^{k+1}, \widetilde{U}^{k-1})| \le C, \quad |g(u^{k+1}, u^{k-1}) - g(\widetilde{U}^{k+1}, \widetilde{U}^{k-1})| \le C(|\widetilde{e}^{k+1}| + |\widetilde{e}^{k-1}|). \tag{72}$$

It follows from (72) that

$$|g(u_i^{k+1}, u_i^{k-1})\phi_i^k - g(\widetilde{U}_i^{k+1}, \widetilde{U}_i^{k-1})\widetilde{\Phi}_i^k| \le C(|\widetilde{e}^{k+1}| + |\widetilde{e}^{k-1}| + |\widetilde{\xi}^k|). \tag{73}$$

Note that

$$\begin{aligned}&f_B(|u_i^k|^2)\mu_t u_i^k - f_B(|\widetilde{U}_i^k|^2)\mu_t \widetilde{U}_i^k \\ &= [f_B(|u_i^k|^2) - f_B(|\widetilde{U}_i^k|^2)]\mu_t u_i^k + f_B(|\widetilde{U}_i^k|^2)\mu_t \widetilde{e}_i^k.\end{aligned} \tag{74}$$

Journal Pre-proof

Invoking the definition of $f_B(s)$ and (60), the following inequalities hold:

$$\begin{aligned}&|f_B(|u_i^k|^2)\mu_t u_i^k - f_B(|\widetilde{U}_i^k|^2)\mu_t \widetilde{U}_i^k| \le C(|\widetilde{e}_i^k| + |\widetilde{e}_i^{k-1}| + |\widetilde{e}_i^{k+1}|),\\ &|f_B(|u_i^k|^2) - f_B(|\widetilde{U}_i^k|^2)| \le \sqrt{C_B}|\widetilde{e}_i^k|.\end{aligned} \tag{75}$$

Remark that

$$\sum_{k=1}^{K}(v^k, 2\Delta t\mathcal{D}_t w^k) = (v^K, w^{K+1}) + (v^{K+1}, w^K) - (v^1, w^0) - (v^0, w^1) - \sum_{k=1}^{K}(w^k, 2\Delta t\mathcal{D}_t v^k). \tag{76}$$

Applying (76) to the third part on the right hand side of (70), we further obtain

$$\sum_{k=1}^{K}(\widetilde{r}^k, 2\Delta t\mathcal{D}_t\widetilde{\xi}^k) = (\widetilde{r}^K, \widetilde{\xi}^{K+1}) + (\widetilde{r}^{K+1}, \widetilde{\xi}^K) - (\widetilde{r}^1, \widetilde{\xi}^0) - (\widetilde{r}^0, \widetilde{\xi}^1) - \sum_{k=1}^{K}(\widetilde{\xi}^k, 2\Delta t\mathcal{D}_t\widetilde{r}^k), \tag{77}$$

where $\widetilde{r}_i^k := f_B(|u_i^k|^2) - f_B(|\widetilde{U}_i^k|^2)$.

In the following, we make the estimation of the fourth part on the right hand side of (77). By using (65) and (73), and some subtle calculations, we further deduce that

$$\begin{aligned}2\Delta t\mathcal{D}_t\widetilde{r}_i^k &= 4\Delta t g(u_i^{k+1}, u_i^{k-1})\mathcal{D}_t u_i^k - 4\Delta t g(\widetilde{U}_i^{k+1}, \widetilde{U}_i^{k-1})\mathcal{D}_t\widetilde{U}_i^k\\ &= 4\Delta t g(\widetilde{U}_i^{k+1}, \widetilde{U}^{k-1})\mathcal{D}_t\widetilde{e}_i^k + 4\Delta t[g(u_i^{k+1}, u_i^{k-1}) - g(\widetilde{U}_i^{k+1}, \widetilde{U}_i^{k-1})]\mathcal{D}_t u_i^k\\ &= 4\Delta t g(\widetilde{U}_i^{k+1}, \widetilde{U}_i^{k-1})(-\mu_t\widetilde{\eta}_i^k + {R_1}_i^k) + 4\Delta t[g(u_i^{k+1}, u_i^{k-1}) - g(\widetilde{U}_i^{k+1}, \widetilde{U}_i^{k-1})]\mathcal{D}_t u_i^k\\ &\le C\Delta t(|\widetilde{\eta}_i^{k+1}| + |\widetilde{\eta}_i^{k-1}| + |{R_1}_i^k|) + C\Delta t(|\widetilde{e}_i^{k-1}| + |\widetilde{e}_i^{k+1}|)\|\frac{\partial u}{\partial t}(\cdot, t_k)\|_\infty.\end{aligned} \tag{78}$$

For ease of notation, we introduce

$$\begin{aligned}\mathcal{F}^k = &2(\|\widetilde{\eta}^{k+1}\|^2 + \|\widetilde{\eta}^k\|^2) + 4C_B(\|\Lambda^\gamma\widetilde{e}^{k+1}\|^2 + \|\Lambda^\gamma\widetilde{e}^k\|^2) + 4C_B(\|\widetilde{e}^{k+1}\|^2 + \|\widetilde{e}^k\|^2)\\ &+(\|\widetilde{\xi}^{k+1}\|^2 + \|\widetilde{\xi}^k\|^2) + (\|\delta_x\widetilde{\theta}^{k+1}\|^2 + \|\delta_x\widetilde{\theta}^k\|^2).\end{aligned} \tag{79}$$

Multiplying (69) by $4\Delta t$ and summing the result to (70) multiplied by $4\Delta t$, by using the definition of $\mathcal{F}^k$ and $\widetilde{r}_i^k$, summing up k from 1 to K, we further obtain

$$\begin{aligned}\mathcal{F}^K - \mathcal{F}^0 = &\Delta t\sum_{k=1}^{K}[8(R_1^k, \mathcal{D}_t\widetilde{\eta}^k) - 16C_B(R_2^k, \mathcal{D}_t\widetilde{e}^k) + 4(R_3^k, \mathcal{D}_t\widetilde{\theta}^k) - 4(R_4^k, \mathcal{D}_t\widetilde{\xi}^k)]\\ &-16C_B\Delta t\sum_{k=1}^{K}(g(u^{k+1}, u^{k-1})\phi^k - g(\widetilde{U}^{k+1}, \widetilde{U}^{k-1})\widetilde{\Phi}^k, \mathcal{D}_t\widetilde{e}^k)\\ &-16C_B\Delta t\sum_{k=1}^{K}(f_B(|u^k|^2)\mu_t u^k - f_B(|\widetilde{U}^k|^2)\mu_t\widetilde{U}^k, \mathcal{D}_t\widetilde{e}^k) - 4\Delta t\sum_{k=1}^{K}(\widetilde{r}^k, \mathcal{D}_t\widetilde{\xi}^k).\end{aligned} \tag{80}$$

For the second sum term on the right hand side of (80), by using (65) and (73), with Cauchy-Schwartz inequality at hand, we have

$$\begin{aligned}&-16C_B\Delta t\sum_{k=1}^{K}(g(u^{k+1}, u^{k-1})\phi^k - g(\widetilde{U}^{k+1}, \widetilde{U}^{k-1})\widetilde{\Phi}^k, \mathcal{D}_t\widetilde{e}^k)\\ &= -16\Delta t\sum_{k=1}^{K}(g(u^{k+1}, u^{k-1})\phi^k - g(\widetilde{U}^{k+1}, \widetilde{U}^{k-1})\widetilde{\Phi}^k, -\mu_t\widetilde{\eta}^k + {R_1}^k)\\ &\le C\Delta t\sum_{k=1}^{K}(4C_B\|\widetilde{e}^{k-1}\|^2 + \|\widetilde{\xi}^k\|^2 + 4C_B\|\widetilde{e}^{k+1}\|^2 + \|\widetilde{\eta}^{k-1}\|^2 + \|\widetilde{\eta}^{k+1}\|^2) + C\Delta t\sum_{k=1}^{K}\|R_1^k\|^2.\end{aligned} \tag{81}$$

Journal Pre-proof

For the third sum term on the right hand side of (80), by using (65), (75) and Cauchy-Schwartz inequality, we obtain

$$\begin{aligned}
&-16\Delta t\sum_{k=1}^{K}(f_B(|u^k|^2)\mu_t u^k - f_B(|\widetilde{U}^k|^2)\mu_t\widetilde{U}^k, \mathcal{D}_t\widetilde{e}^k)\\
&= -16\Delta t\sum_{k=1}^{K}(f_B(|u^k|^2)\mu_t u^k - f_B(|\widetilde{U}^k|^2)\mu_t\widetilde{U}^k, -\mu_t\widetilde{\eta}^k + {R_1}^k)\\
&\le C\Delta t\sum_{k=1}^{K}(\|\widetilde{e}^{k-1}\|^2 + \|\widetilde{e}^k\|^2 + \|\widetilde{e}^{k+1}\|^2 + \|\widetilde{\eta}^{k-1}\|^2 + \|\widetilde{\eta}^{k+1}\|^2) + C\Delta t\sum_{k=1}^{K}\|R_1^k\|^2.
\end{aligned} \tag{82}$$

For the fourth sum term on the right hand side of (80), by using (77)–(78), we have

$$\begin{aligned}
&-4\Delta t\sum_{k=1}^{K}(\widetilde{r}^k, \mathcal{D}_t\widetilde{\xi}^k)\\
&= -2[(\widetilde{r}^K, \widetilde{\xi}^{K+1}) + (\widetilde{r}^{K+1}, \widetilde{\xi}^K) - (\widetilde{r}^1, \widetilde{\xi}^0) - (\widetilde{r}^0, \widetilde{\xi}^1) - \sum_{k=1}^{K}(\widetilde{\xi}^k, 2\Delta t\mathcal{D}_t\widetilde{r}^k)].
\end{aligned} \tag{83}$$

It follows from ε-inequality $ab \le \varepsilon a^2 + \frac{1}{4\varepsilon}b^2$, (75) and (78) that

$$\begin{aligned}
&-2[(\widetilde{r}^K, \widetilde{\xi}^{K+1}) + (\widetilde{r}^{K+1}, \widetilde{\xi}^K)]\\
&\le 2\|\widetilde{r}^K\|^2 + \frac{1}{2}\|\widetilde{\xi}^{K+1}\|^2 + 2\|\widetilde{r}^{K+1}\|^2 + \frac{1}{2}\|\widetilde{\xi}^K\|^2\\
&\le 2C_B\|\widetilde{e}^K\|^2 + \frac{1}{2}\|\widetilde{\xi}^{K+1}\|^2 + 2C_B\|\widetilde{e}^{K+1}\|^2 + \frac{1}{2}\|\widetilde{\xi}^K\|^2,
\end{aligned} \tag{84}$$

$$\begin{aligned}
&-2[-(\widetilde{r}^1, \widetilde{\xi}^0) - (\widetilde{r}^0, \widetilde{\xi}^1)]\\
&\le \|\widetilde{r}^1\|^2 + \|\widetilde{\xi}^0\|^2 + \|\widetilde{r}^0\|^2 + \|\widetilde{\xi}^1\|^2\\
&\le C\|\widetilde{e}^1\|^2 + \|\widetilde{\xi}^1\|^2,
\end{aligned} \tag{85}$$

$$\begin{aligned}
&2\sum_{k=1}^{K}(\widetilde{\xi}^k, 2\Delta t\mathcal{D}_t\widetilde{r}^k)\\
&\le C\Delta t\sum_{k=1}^{K}(\|\widetilde{\xi}^k\|^2 + \|\widetilde{\eta}^{k+1}\|^2 + \|\widetilde{\eta}^{k-1}\|^2 + 4C_B\|\widetilde{e}^{k+1}\|^2 + 4C_B\|\widetilde{e}^{k-1}\|^2) + C\Delta t\sum_{k=1}^{K}\|R_1^k\|^2.
\end{aligned} \tag{86}$$

Plugging (84)–(86) into (83) yields

$$\begin{aligned}
&-4\Delta t\sum_{k=1}^{K}(\widetilde{r}^k, \mathcal{D}_t\widetilde{\xi}^k)\\
&\le 2C_B\|\widetilde{e}^K\|^2 + \frac{1}{2}\|\widetilde{\xi}^{K+1}\|^2 + 2C_B\|\widetilde{e}^{K+1}\|^2 + \frac{1}{2}\|\widetilde{\xi}^K\|^2\\
&\quad + C\Delta t\sum_{k=1}^{K}(\|\widetilde{\xi}^k\|^2 + \|\widetilde{\eta}^{k+1}\|^2 + \|\widetilde{\eta}^{k-1}\|^2 + 4C_B\|\widetilde{e}^{k+1}\|^2 + 4C_B\|\widetilde{e}^{k-1}\|^2)\\
&\quad + C(\Delta t^2 + h^2),
\end{aligned} \tag{87}$$

where Lemma 5 and (59) are employed.

Journal Pre-proof

In what follows, we shall do the estimations of the first sum term on the right hand side of (80).

After some calculations, the following is valid.

$$\sum_{k=1}^{K}(R_1^k,\mathcal{D}_t\widetilde{\eta}^k)=\frac{1}{2\Delta t}[(R_1^{K-1},\widetilde{\eta}^K)+(R_1^K,\widetilde{\eta}^{K+1})-(R_1^1,\widetilde{\eta}^0)-(R_1^2,\widetilde{\eta}^1)]-\sum_{k=2}^{K-1}(\mathcal{D}_tR_1^k,\widetilde{\eta}^k), \quad (88)$$

$$\sum_{k=1}^{K}(R_2^k,\mathcal{D}_t\widetilde{e}^k)=\frac{1}{2\Delta t}[(R_2^{K-1},\widetilde{e}^K)+(R_2^K,\widetilde{e}^{K+1})-(R_2^1,\widetilde{e}^0)-(R_2^2,\widetilde{e}^1)]-\sum_{k=2}^{K-1}(\mathcal{D}_tR_2^k,\widetilde{e}^k), \quad (89)$$

$$\sum_{k=1}^{K}(R_3^k,\mathcal{D}_t\widetilde{\theta}^k)=\frac{1}{2\Delta t}[(R_3^{K-1},\widetilde{\theta}^K)+(R_3^K,\widetilde{\theta}^{K+1})-(R_3^1,\widetilde{\theta}^0)-(R_3^2,\widetilde{\theta}^1)]-\sum_{k=2}^{K-1}(\mathcal{D}_tR_3^k,\widetilde{\theta}^k), \quad (90)$$

$$\sum_{k=1}^{K}(R_4^k,\mathcal{D}_t\widetilde{\xi}^k)=\frac{1}{2\Delta t}[(R_4^{K-1},\widetilde{\xi}^K)+(R_4^K,\widetilde{\xi}^{K+1})-(R_4^1,\widetilde{\xi}^0)-(R_4^2,\widetilde{\xi}^1)]-\sum_{k=2}^{K-1}(\mathcal{D}_tR_4^k,\widetilde{\xi}^k). \quad (91)$$

Using ε-inequality $ab\le\varepsilon a^2+\frac{1}{4\varepsilon}b^2$, (88)–(91) and Lemma 5, by clever calculations, we can deduce that

$$\begin{aligned}
&8\Delta t\sum_{k=1}^{K}(R_1^k,\mathcal{D}_t\widetilde{\eta}^k)\\
&\le C\|R_1^{K-1}\|^2+\frac{1}{2}\|\widetilde{\eta}^K\|^2+C\|R_1^K\|^2+\frac{1}{2}\|\widetilde{\eta}^{K+1}\|^2+C\|R_1^1\|^2+C\|R_1^2\|^2\\
&\quad+C\|\widetilde{\eta}^1\|^2+C\Delta t\sum_{k=2}^{K-1}\|\mathcal{D}_tR_1^k\|^2+C\Delta t\sum_{k=2}^{K-1}\|\widetilde{\eta}^k\|^2\\
&\le\frac{1}{2}\|\widetilde{\eta}^K\|^2+\frac{1}{2}\|\widetilde{\eta}^{K+1}\|^2+C\Delta t\sum_{k=2}^{K-1}\|\widetilde{\eta}^k\|^2+C(\Delta t^2+h^2)^2.
\end{aligned} \quad (92)$$

Similarly, we derive that

$$\begin{aligned}
&-16C_B\Delta t\sum_{k=1}^{K}(R_2^k,\mathcal{D}_t\widetilde{e}^k)\\
&\le C\|R_2^{K-1}\|^2+\frac{1}{2}C_B\|\widetilde{e}^K\|^2+C\|R_2^K\|^2+\frac{1}{2}C_B\|\widetilde{e}^{K+1}\|^2+C\|R_2^1\|^2+C\|R_2^2\|^2\\
&\quad+C\|\widetilde{e}^1\|^2+C\Delta t\sum_{k=2}^{K-1}\|\mathcal{D}_tR_2^k\|^2+C\Delta t\sum_{k=2}^{K-1}\|\widetilde{e}^k\|^2\\
&\le\frac{1}{2}C_B\|\widetilde{e}^K\|^2+\frac{1}{2}C_B\|\widetilde{e}^{K+1}\|^2+C\Delta t\sum_{k=2}^{K-1}\|\widetilde{e}^k\|^2+C(\Delta t^2+h^2)^2,
\end{aligned} \quad (93)$$

$$\begin{aligned}
&4\Delta t\sum_{k=1}^{K}(R_3^k,\mathcal{D}_t\widetilde{\theta}^k)\\
&\le C\|R_3^{K-1}\|^2+\frac{1}{2}\|\delta_x\widetilde{\theta}^K\|^2+C\|R_3^K\|^2+\frac{1}{2}\|\delta_x\widetilde{\theta}^{K+1}\|^2+C\|R_3^1\|^2+C\|R_3^2\|^2\\
&\quad+C\|\widetilde{\theta}^1\|^2+C\Delta t\sum_{k=2}^{K-1}\|\mathcal{D}_tR_3^k\|^2+C\Delta t\sum_{k=2}^{K-1}\|\delta_x\widetilde{\theta}^k\|^2\\
&\le\frac{1}{2}\|\delta_x\widetilde{\theta}^K\|^2+\frac{1}{2}\|\delta_x\widetilde{\theta}^{K+1}\|^2+C\Delta t\sum_{k=2}^{K-1}\|\delta_x\widetilde{\theta}^k\|^2+C(\Delta t^2+h^2)^2,
\end{aligned} \quad (94)$$

Journal Pre-proof

where the poincáre inequality [51] is invoked to (94).

$$\begin{aligned}
&-4\Delta t\sum_{k=1}^{K}(R_4^k,\mathcal{D}_t\widetilde{\xi}^k)\\
&\le C\|R_4^{K-1}\|^2+\frac{1}{4}\|\widetilde{\xi}^K\|^2+C\|R_4^K\|^2+\frac{1}{4}\|\widetilde{\xi}^{K+1}\|^2+C\|R_4^1\|^2+C\|R_4^2\|^2\\
&\quad+C\|\widetilde{\xi}^1\|^2+C\Delta t\sum_{k=2}^{K-1}\|\mathcal{D}_tR_4^k\|^2+C\Delta t\sum_{k=2}^{K-1}\|\widetilde{\xi}^k\|^2\\
&\le\frac{1}{4}\|\widetilde{\xi}^K\|^2+\frac{1}{4}\|\widetilde{\xi}^{K+1}\|^2+C\Delta t\sum_{k=2}^{K-1}\|\widetilde{\xi}^k\|^2+C(\Delta t^2+h^2)^2.
\end{aligned}\tag{95}$$

Noticing that by (87), (92)-(95) and the definition of $\mathcal{F}^k$, we conclude

$$\begin{aligned}
&2C_B\|\widetilde{e}^K\|^2+\frac{1}{2}\|\widetilde{\xi}^{K+1}\|^2+2C_B\|\widetilde{e}^{K+1}\|^2+\frac{1}{2}\|\widetilde{\xi}^K\|^2\\
&\quad+\frac{1}{2}\|\widetilde{\eta}^K\|^2+\frac{1}{2}\|\widetilde{\eta}^{K+1}\|^2+\frac{1}{2}C_B\|\widetilde{e}^K\|^2+\frac{1}{2}C_B\|\widetilde{e}^{K+1}\|^2\\
&\quad+\frac{1}{2}\|\delta_x\widetilde{\theta}^K\|^2+\frac{1}{2}\|\delta_x\widetilde{\theta}^{K+1}\|^2+\frac{1}{4}\|\widetilde{\xi}^K\|^2+\frac{1}{4}\|\widetilde{\xi}^{K+1}\|^2\\
&\le\frac{3}{4}\mathcal{F}^K.
\end{aligned}\tag{96}$$

Substituting (87) and (92)–(95) into (80), invoking (96), (59) and the definition of $\mathcal{F}^k$, we arrive at

$$\begin{aligned}
\mathcal{F}^K&\le 4\mathcal{F}^0+4C\Delta t\sum_{k=1}^{K}(\mathcal{F}^k+\mathcal{F}^{k-1})+C(\Delta t^2+h^2)^2\\
&\le 4\mathcal{F}^0+8C\Delta t\sum_{k=0}^{K}\mathcal{F}^k+C(\Delta t^2+h^2)^2\\
&\le 8C\Delta t\sum_{k=0}^{K}\mathcal{F}^k+C(\Delta t^2+h^2)^2.
\end{aligned}\tag{97}$$

An application of the discrete Gronwall lemma [51, 53, 54] to (97), we have

$$\mathcal{F}^K\le\exp(8CT)C(\Delta t^2+h^2)^2.\tag{98}$$

Using the definition of $\mathcal{F}^k$, Lemma 3 and Lemma 4, we achieve

$$\begin{aligned}
&\|\Lambda^\gamma\widetilde{e}^{K+1}\|+\|\widetilde{e}^{K+1}\|+\|\widetilde{\eta}^{K+1}\|+\|\widetilde{\xi}^{K+1}\|+\|\delta_x\widetilde{\theta}^{K+1}\|\le C(\Delta t^2+h^2),\\
&\|\widetilde{e}^{K+1}\|_\infty\le C\|\widetilde{e}^{K+1}\|_{H^{\frac{\gamma}{2}}}\le C(\Delta t^2+h^2),
\end{aligned}\tag{99}$$

which further indicates that

$$\|\widetilde{U}^k\|_\infty\le\|u^k\|_\infty+\|\widetilde{e}^k\|_\infty\le M_1+C(\Delta t^2+h^2).\tag{100}$$

Therefore, we further attain from (100)

$$\|\widetilde{U}^k\|_\infty\le M_1+1=\sqrt{B},\quad 0\le k\le N,\tag{101}$$

Journal Pre-proof

provided that $\Delta t_0 > 0$ and $h_0 > 0$ are small enough.

Using $f_B(s)$, we have $f_B(\|\widetilde{U}^k\|^2) = \|\widetilde{U}^k\|^2$, which implies that the underlying algorithm (61)–(64) is isovalent to (19)–(22), that is,

$$(\widetilde{U}^k, \widetilde{V}^k, \widetilde{\Phi}^k, \widetilde{\Psi}^k) = (U^k, V^k, \Phi^k, \Psi^k), \quad (\widetilde{e}^k, \widetilde{\eta}^k, \widetilde{\xi}^k, \widetilde{\theta}^k) = (e^k, \eta^k, \xi^k, \theta^k). \tag{102}$$

Collecting (99) and (101) further indicates the claimed results. Here we complete the proof. □

Utilizing the arguments analogous to those applied in the proof of Theorem 2, the following stability result can be also shown rigidly.

Theorem 3 Provided that the conditions of Theorem 2 are valid, the numerical solutions of underlying scheme (19)–(30) are unconditionally stable with regards to initial values.

Similarly, as in the proof of Theorem 2, we can obtain error estimate for the energy of the proposed scheme (19)–(30) in the discrete level as

Theorem 4 Under the conditions of Theorem 2, we have

$$\|E^k - E(t_k)\|_\infty \leq C(\Delta t^2 + h^2), \ \ 1 \leq k \leq N-1.$$

4 Establishment and analysis of a spatial fourth-order linear difference scheme with energy conservative property

As discussed above, we have proposed a second-order linearized implicit difference scheme with energy conservation property for fractional KGZ system and analyze the corresponding error estimations. To enhance the computational efficiency, we present a spatial fourth-order linear difference scheme with energy conservation property for fractional KGZ system. The following lemmas are useful in the derivation and theoretical analysis of the desired linear conservative difference scheme.

Lemma 6 (cf. [41]) Assume that $u \in \mathcal{C}^{4+\gamma}(\mathbb{R}) := \left\{u | \int_{-\infty}^{\infty}(1+|\xi|)^{4+\gamma}|\hat{u}(\xi)|d\xi < \infty\right\}$, then for a fixed h, we have

$$-\delta_h^\gamma u(x) = -(-\Delta)^{\frac{\gamma}{2}}u(x) + \mathcal{O}(h^4), \ \ 1 < \gamma \leq 2,$$

where $\delta_h^\gamma u(x) = \frac{4}{3}\widetilde{\delta}_h u(x) - \frac{1}{3}\widetilde{\delta}_{2h} u(x) = \frac{1}{h^\gamma}\sum\limits_{m=-\infty}^{+\infty}\hat{q}_m^{(\gamma)}u(x-mh)$, $\widetilde{\delta}_h^\gamma u(x) = \frac{1}{h^\gamma}\sum\limits_{m=-\infty}^{+\infty} q_m^{(\gamma)}u(x-mh)$,

$$\hat{q}_m^{(\gamma)} = \begin{cases} \dfrac{4}{3}q_m^{(\gamma)} - \dfrac{1}{3\cdot 2^\gamma}q_{\frac{m}{2}}^{(\gamma)}, & k \ \text{ is even}, \\ \dfrac{4}{3}q_m^{(\gamma)}, & k \ \text{ is odd}, \end{cases}$$

$q_0^{(\gamma)} = \Gamma(\gamma+1)/\Gamma(\gamma/2+1)^2$, $q_{m+1}^{(\gamma)} = [1-(\gamma+1)/(\gamma/1+m+1)]q_m^{(\gamma)}$, $m = \mp 1, \mp 2, \ldots$.

Lemma 7 There exists a unique linear operator $\widetilde{\Lambda}^\gamma : V_h \to V_h$, such that $(\delta_h^\gamma u, v) = (\widetilde{\Lambda}^\gamma u, \widetilde{\Lambda}^\gamma v)$ for $\forall u, v \in V_h$.

Journal Pre-proof

4.1 Derivation of the fourth-order linear energy conservative finite difference method

Here, to construct fourth-order difference algorithm, for $g = (g_0, g_1, \ldots, g_M)$, introducing the average operator as [51]

$$\mathcal{A}g_i = \frac{1}{12}g_{i+1} + \frac{5}{6}g_i + \frac{1}{12}g_{i-1},$$

and employing the Taylor expansion with Maclaurin remainder further imply

$$\delta_x^2\psi_i^k = \mathcal{A}\frac{\partial^2\psi_i^k}{\partial x^2} - \frac{h^4}{240}\frac{\partial^6\psi_i^k}{\partial x^6} + \mathcal{O}(h^6). \tag{103}$$

By virtue of Lemma 6 and leap-frog scheme for the approximations of (15)–(16) in space and time directions, and meanwhile using compact finite difference scheme to approximate space direction and leap-frog scheme to solve time direction for (17)–(18), we create the difference algorithm for the transformed system (7)–(12) as

$$\mathcal{D}_t U_i^k = -\mu_t V_i^k, \tag{104}$$

$$\mathcal{D}_t V_i^k = \delta_h^\gamma \mu_t U_i^k + \mu_t U_i^k + \mu_t U_i^k \Phi_i^k + |U_i^k|^2 \mu_t U_i^k, \tag{105}$$

$$\mathcal{A}\mathcal{D}_t \Phi_i^k = \delta_x^2 \mu_t \Psi_i^k, \tag{106}$$

$$\mathcal{D}_t \Psi_i^k = \mu_t \Phi_i^k + |U_i^k|^2. \tag{107}$$

Here, invoking (103), we establish the following modified Crank-Nicolson spatial fourth-order difference scheme to compute U_i^1, V_i^1, Φ_i^1 and Ψ_i^1 as

$$\delta_t U_i^{\frac{1}{2}} = -V_i^{\frac{1}{2}}, \tag{108}$$

$$\delta_t V_i^{\frac{1}{2}} = \delta_h^\gamma U_i^{\frac{1}{2}} + U_i^{\frac{1}{2}} + U_i^{\frac{1}{2}} \Phi_i^{(\frac{1}{2})} + |U_i^{(\frac{1}{2})}|^2 U_i^{\frac{1}{2}}, \tag{109}$$

$$\mathcal{A}\delta_t \Phi_i^{\frac{1}{2}} = \delta_x^2 \Psi_i^{\frac{1}{2}}, \tag{110}$$

$$\delta_t \Psi_i^{\frac{1}{2}} = \Phi_i^{\frac{1}{2}} + |U_i^{(\frac{1}{2})}|^2, \tag{111}$$

where $U^{(\frac{1}{2})}$ and $\Phi^{(\frac{1}{2})}$ are calculated by (27) and (28).

And the corresponding initial and boundary conditions are given as follows:

$$U_i^0 = u_0(x_i),\ V_i^0 = v_0(x_i),\ \Phi_i^0 = \phi_0(x_i),\ \Psi_i^0 = \widetilde{\Psi}_i^0 \tag{112}$$

$$U_0^k = U_M^k = 0,\ V_0^k = V_M^k = 0,\ \Phi_0^k = \Phi_M^k = 0,\ \Psi_0^k = \Psi_M^k = 0, \tag{113}$$

where Ψ_i^0 is ascertained by the following spatial fourth-order difference scheme

$$\begin{aligned} &\delta_x^2 \Psi_i^0 = \mathcal{A}\phi_1(x_i),\ 1 \le i \le M-1, \\ &\Psi_0^0 = \Psi_M^0 = 0. \end{aligned} \tag{114}$$

Journal Pre-proof

Define vectors

$$U^k = (U_1^k, U_2^k, \ldots, U_{M-1}^k)^T, \;\; V^k = (V_1^k, V_2^k, \ldots, V_{M-1}^k)^T,$$
$$\Phi^k = (\Phi_1^k, \Phi_2^k, \ldots, \Phi_{M-1}^k)^T, \;\; \Psi^k = (\Psi_1^k, \Psi_2^k, \ldots, \Psi_{M-1}^k)^T,$$

and matrices

$$\mathrm{H} = \frac{1}{12}\begin{pmatrix} 10 & 1 & & & \\ 1 & 10 & 1 & & \\ & \ddots & \ddots & \ddots & \\ & & 1 & 10 & 1 \\ & & & 1 & 10 \end{pmatrix}_{(M-1)\times(M-1)},$$

$$\mathrm{B} = \frac{1}{h^2}\begin{pmatrix} 2 & -1 & & & \\ -1 & 2 & -1 & & \\ & \ddots & \ddots & \ddots & \\ & & -1 & 2 & -1 \\ & & & -1 & 2 \end{pmatrix}_{(M-1)\times(M-1)},$$

$$\mathrm{Q}^{(\gamma)} = \frac{1}{h^\gamma}\begin{pmatrix} \hat{q}_0^{(\gamma)} & \hat{q}_{-1}^{(\gamma)} & \hat{q}_{-2}^{(\gamma)} & \cdots & \hat{q}_{-M+2}^{(\gamma)} \\ \hat{q}_1^{(\gamma)} & \hat{q}_0^{(\gamma)} & \hat{q}_{-1}^{(\gamma)} & \cdots & \hat{q}_{-M+3}^{(\gamma)} \\ \hat{q}_2^{(\gamma)} & \hat{q}_1^{(\gamma)} & \hat{q}_0^{(\gamma)} & \cdots & \hat{q}_{-M+4}^{(\gamma)} \\ \vdots & \vdots & \vdots & \ddots & \vdots \\ \hat{q}_{M-2}^{(\gamma)} & \hat{q}_{M-3}^{(\gamma)} & \hat{q}_{M-4}^{(\gamma)} & \cdots & \hat{q}_0^{(\gamma)} \end{pmatrix}_{(M-1)\times(M-1)}.$$

Then the vector form of the underlying difference algorithm (104)–(114) is listed as

$$\mathcal{D}_t U^k = -\mu_t V^k, \tag{115}$$

$$\mathcal{D}_t V^k = \mathrm{Q}^{(\gamma)}\mu_t U^k + \mu_t U^k + \mu_t U^k \cdot \Phi^k + |U^k|_\cdot^2 \cdot \mu_t U^k, \tag{116}$$

$$\mathrm{H}\mathcal{D}_t \Phi^k = -\mathrm{B}\mu_t \Psi^k, \tag{117}$$

$$\mathcal{D}_t \Psi^k = \mu_t \Phi^k + |U^k|^2, \tag{118}$$

$$\delta_t U^{\frac{1}{2}} = -V^{\frac{1}{2}}, \tag{119}$$

$$\delta_t V^{\frac{1}{2}} = \mathrm{Q}^{(\gamma)} U^{\frac{1}{2}} + U^{\frac{1}{2}} + U^{\frac{1}{2}} \cdot \Phi^{(\frac{1}{2})} + |U^{(\frac{1}{2})}|_\cdot^2 \cdot U^{\frac{1}{2}}, \tag{120}$$

$$\mathrm{H}\delta_t \Phi^{\frac{1}{2}} = -\mathrm{B}\Psi^{\frac{1}{2}}, \tag{121}$$

$$\delta_t \Psi^{\frac{1}{2}} = \Phi^{\frac{1}{2}} + |U^{(\frac{1}{2})}|_\cdot^2, \tag{122}$$

$$U_i^0 = u_0(x_i), \;\; V_i^0 = v_0(x_i), \;\; \Phi_i^0 = \phi_0(x_i), \;\; \Psi_i^0 = \widetilde{\Psi}_i^0, \tag{123}$$

$$U_0^k = U_M^k = 0, \;\; V_0^k = V_M^k = 0, \;\; \Phi_0^k = \Phi_M^k = 0, \;\; \Psi_0^k = \Psi_M^k = 0, \tag{124}$$

where $|U^k|_\cdot^2 = |U^k| \cdot |U^k|$ and "$\cdot$" represents the component multiplication between two vectors.

Journal Pre-proof

Note that H is a real-value symmetric positive definite (SPD) matrix, and hence there exists a real-value SPD matrix M, such that $\mathrm{M} = \mathrm{H}^{-1}$. Then (115)–(124) is equivalent to

$$\mathcal{D}_t U^k = -\mu_t V^k, \tag{125}$$

$$\mathcal{D}_t V^k = \mathrm{Q}^{(\gamma)} \mu_t U^k + \mu_t U^k + \mu_t U^k \cdot \Phi^k + |U|.^2 \cdot \mu_t U^k, \tag{126}$$

$$\mathcal{D}_t \Phi_i^k = -\mathrm{MB} \mu_t \Psi^k, \tag{127}$$

$$\mathcal{D}_t \Psi^k = \mu_t \Phi^k + |U^k|^2, \tag{128}$$

$$\delta_t U^{\frac{1}{2}} = -V^{\frac{1}{2}}, \tag{129}$$

$$\delta_t V^{\frac{1}{2}} = \mathrm{Q}^{(\gamma)} U^{\frac{1}{2}} + U^{\frac{1}{2}} + U^{\frac{1}{2}} \cdot \Phi^{(\frac{1}{2})} + |U^{(\frac{1}{2})}|.^2 \cdot U^{\frac{1}{2}}, \tag{130}$$

$$\delta_t \Phi^{\frac{1}{2}} = -\mathrm{MB} \Psi^{\frac{1}{2}}, \tag{131}$$

$$\delta_t \Psi^{\frac{1}{2}} = \Phi^{\frac{1}{2}} + |U^{(\frac{1}{2})}|.^2, \tag{132}$$

$$U_i^0 = u_0(x_i), \;\; V_i^0 = v_0(x_i), \;\; \Phi_i^0 = \phi_0(x_i), \;\; \Psi_i^0 = \widetilde{\Psi}_i^0, \tag{133}$$

$$U_0^k = U_M^k = 0, \;\; V_0^k = V_M^k = 0, \;\; \Phi_0^k = \Phi_M^k = 0, \;\; \Psi_0^k = \Psi_M^k = 0. \tag{134}$$

Remark 2 Employing the Cholesky decomposition, the property of H and B, it is easy to check that there exists a matrix R fulfilling $(\mathrm{MB}U^k, U^k) = \|\mathrm{R}U^k\|^2$.

4.2 Theoretical analysis of the spatial fourth-order difference scheme

This subsection is suggested for the discrete energy conservation property of the proposed scheme (125)–(134).

Theorem 5 Let U_i^k, V_i^k, Φ_i^k and Ψ_i^k be the numerical solutions of (125)–(134). Then (125)–(134) fulfills energy conservation property, that is,

$$\widetilde{E}^k = \widetilde{E}^0, \tag{135}$$

where

$$\begin{aligned}\widetilde{E}^k = &(\|V^{k+1}\|^2 + \|V^k\|^2) + (\|\widetilde{\Lambda}^\gamma U^{k+1}\|^2 + \|\widetilde{\Lambda}^\gamma U^k\|^2) + (\|U^{k+1}\|^2 + \|U^k\|^2) \\ &+ \frac{1}{2}(\|\mathrm{R}\Psi^{k+1}\|^2 + \|\mathrm{R}\Psi^k\|^2) + \frac{1}{2}(\|\Phi^{k+1}\|^2 + \|\Phi^k\|^2) \\ &+ \sum_{i=1}^{M-1} |U_i^k|^2 |U_i^{k+1}|^2 h + \sum_{i=1}^{M-1} [|U_i^{k+1}|^2 \Phi_i^k + |U_i^k|^2 \Phi_i^{k+1}] h\end{aligned}$$

is the associated discrete energy.

Proof. Similar to the proof of Theorem 1, using Lemma 7 and Remark 2, we can attain the claimed results.

Analogous to the arguments and techniques used in the proof of Theorem 2, we can deduce the following convergence and stability of (125)–(134). The detailed proof is omitted avoid lengthy.

Theorem 6 Assume that $u(x,t)$, $v(x,t)$, $\phi(x,t)$ and $\psi(x,t)$ are the exact solutions of the transformed system (7)–(10). Let U_i^k, V_i^k, Φ_i^k and Ψ_i^k be the numerical solutions of (125)–(134).

Journal Pre-proof

Then as Δt and h are sufficiently small, the difference algorithm (125)–(134) fulfills the error estimates

$$\|e^k\|_\infty \leq C(\Delta t^2 + h^4), \quad \max_{0\leq k\leq N}\{\|e^k\|, \|\eta^k\|, \|\xi^k\|, \|\delta_x\theta^k\|\} \leq C(\Delta t^2 + h^4). \tag{136}$$

Theorem 7 Under the conditions of Theorem 6, the numerical solutions of underlying scheme (125)–(134) are unconditionally stable for initial data.

Theorem 8 Under the conditions of Theorem 6, we obtain

$$\|\widetilde{E}^k - E(t_k)\|_\infty \leq C(\Delta t^2 + h^4), \ \ 1 \leq k \leq N-1.$$

Remark 3 The presented difference schemes in this paper can be extended to simulate the following generalized KGZ system with $p > 1$

$$\begin{cases} \dfrac{\partial^2 u}{\partial t^2} + (-\Delta)^{\frac{\gamma}{2}} u + u + u\phi + |u|^{2p}u = 0, \ \ x \in \mathbb{R}, \ \ 0 < t \leq T, \\ \dfrac{\partial^2 \phi}{\partial t^2} - \dfrac{\partial^2 \phi}{\partial x^2} - \dfrac{\partial^2 |u|^{2p}}{\partial x^2} = 0, \ \ x \in \mathbb{R}, \ \ 0 < t \leq T, \end{cases} \tag{137}$$

equipped with the associated initial and boundary conditions.

5 Numerical experiments

In this section, some numerical examples are performed to substantiate the effectiveness and dynamical behaviors of the suggested algorithms. The L^∞-norm errors of numerical solutions at time $T = N\Delta t$ and the error of energy at time level k are denoted by

$$Err_u(h, \Delta t) = \|e^N\|_\infty, \quad Err_v(h, \Delta t) = \|\eta^N\|_\infty,$$
$$Err_\phi(h, \Delta t) = \|\xi^N\|_\infty, \quad Err_\psi(h, \Delta t) = \|\theta^N\|_\infty,$$
$$Err_{energy} = \|E^k - E(t_k)\|_\infty,$$

and define the relative error of invariant of kth time level RE^k by $RE^k = \log_{10} \frac{|E^k - E^0|}{|E^0|}$, where E^k represents the related discrete energy at time level k.

To gauge the accuracy of the proposed schemes, we define the convergence orders as follows:

$$R_{\chi,\Delta t} = \log_2 \frac{Err_\chi(2h, 2\Delta t)}{Err_\chi(h, \Delta t)}, \ \ R_{\chi,h} = \log_2 \frac{Err_\chi(2h, 4\Delta t)}{Err_\chi(h, \Delta t)},$$

where χ denotes u, v, ϕ, ψ and $energy$, respectively. $R_{\chi,\Delta t}$ and $R_{\chi,h}$ represent the temporal and space convergence orders of the numerical solutions to the associated schemes (19)–(30) and (125)–(134), respectively.

Example 1 We shall investigate the numerical approximation to (1)–(3). Note that as $\gamma = 2$, the equations (1)–(3) reduces to the standard KGZ equations, whose exact solutions are provided by [3, 7]

$$u(x, t) = \mu \mathrm{sech}(\rho(x - \vartheta t)) \exp(\mathrm{i}(-\kappa x + \omega t)), \tag{138}$$

Journal Pre-proof

$$\phi(x,t) = \zeta \mathrm{sech}^2(\rho(x-\vartheta t)), \tag{139}$$

where $\mu = \sqrt{\zeta(\vartheta^2-1)}$, $\rho = \pm\sqrt{(\zeta+\mu^2)/[2(\vartheta^2-1)]}$, $\omega = \pm\sqrt{(2+\zeta+\mu^2)/[2(1-\vartheta^2)]}$, $\kappa = \pm\vartheta\omega$. Here, μ and ζ are the amplitudes of the $u(x,t)$ and $\phi(x,t)$ respectively. And also, ρ represents the inverse width of the wave and ϑ denotes the soliton velocity. Remark that $-\kappa x + \omega t$ denotes the phase of the wave with κ as the frequency and ω as the wave number. If $\mu = (\sqrt{10}-\sqrt{2})/2$, $\vartheta = \sqrt{(\sqrt{5}-1)/2}$, and the negative value of ω and positive values for κ and ρ are taken in (138)–(139), the following exact solutions of classical KGZ system can be obtained,

$$u(x,t) = \frac{1}{2}(\sqrt{10}-\sqrt{2})\mathrm{sech}\left(\sqrt{(1+\sqrt{5})/2}x - t\right)\exp\left[\mathrm{i}(\sqrt{2/(1+\sqrt{5})}x - t)\right],$$
$$\phi(x,t) = -2\mathrm{sech}^2\left(\sqrt{(1+\sqrt{5})/2}x - t\right),$$

where $\mathrm{i} = \sqrt{-1}$, and the corresponding initial conditions of fractional KGZ system are taken using the exact solutions.

Table 1: The numerical solutions obtained by the scheme (19)–(30) with different γ at final time $T = 1$ for Example 1.

γ	solution$\backslash(x,t)$	$(-5,1)$	$(0,1)$	$(5,1)$
$\gamma = 1.3$	U	$1.8044e-04-4.7432e-03\mathrm{i}$	$3.1813e-01+6.2055e-01\mathrm{i}$	$5.0260e-03+2.4843e-03\mathrm{i}$
	V	$-1.2184e-02+1.2430e-02\mathrm{i}$	$8.4321e-01-7.6803e-02\mathrm{i}$	$-8.2397e-03-7.4409e-03\mathrm{i}$
	Φ	$6.0837e-05$	$-1.0515e+00$	$-2.0464e-04$
	Ψ	$-9.3321e-01$	$-8.5876e-01$	$9.2080e-01$
$\gamma = 1.5$	U	$-2.5366e-03-4.4973e-03\mathrm{i}$	$2.9539e-01+5.8721e-01\mathrm{i}$	$3.3818e-03+1.5760e-03\mathrm{i}$
	V	$-7.1130e-03+1.2927e-02\mathrm{i}$	$8.3881e-01-3.5275e-02\mathrm{i}$	$-5.6939e-03-5.7798e-03\mathrm{i}$
	Φ	$6.7526e-05$	$-1.0223e+00$	$-2.0364e-04$
	Ψ	$-9.3320e-01$	$-8.7652e-01$	$9.2079e-01$
$\gamma = 1.8$	U	$-6.4611e-03-3.6213e-03\mathrm{i}$	$2.6381e-01+5.3730e-01\mathrm{i}$	$1.3290e-03+8.8768e-05\mathrm{i}$
	V	$8.3523e-04+1.2596e-02\mathrm{i}$	$8.0065e-01+2.0546e-03\mathrm{i}$	$-2.3871e-03-3.0964e-03\mathrm{i}$
	Φ	$7.8365e-05$	$-9.7563e-01$	$-2.0140e-04$
	Ψ	$-9.3319e-01$	$-9.0424e-01$	$9.2079e-01$

Table 2: The numerical solutions derived by the scheme (125)–(134) with different γ at final time $T = 1$ for Example 1.

γ	solution$\backslash(x,t)$	$(-5,1)$	$(0,1)$	$(5,1)$
$\gamma = 1.3$	U	$1.6824e-04-4.7363e-03\mathrm{i}$	$3.1599e-01+6.1808e-01\mathrm{i}$	$5.0239e-03+2.4788e-03\mathrm{i}$
	V	$-1.2157e-02+1.2423e-02\mathrm{i}$	$8.4432e-01-7.3847e-02\mathrm{i}$	$-8.2374e-03-7.4335e-03\mathrm{i}$
	Φ	$6.0658e-05$	$-1.0485e+00$	$-2.0345e-04$
	Ψ	$-9.3321e-01$	$-8.5881e-01$	$9.2080e-01$
$\gamma = 1.5$	U	$-2.5475e-03-4.4889e-03\mathrm{i}$	$2.9363e-01+5.8504e-01\mathrm{i}$	$3.3805e-03+1.5706e-03\mathrm{i}$
	V	$-7.0858e-03+1.2916e-02\mathrm{i}$	$8.3856e-01-3.3715e-02\mathrm{i}$	$-5.6921e-03-5.7722e-03\mathrm{i}$
	Φ	$6.7323e-05$	$-1.0194e+00$	$-2.0246e-04$
	Ψ	$-9.3320e-01$	$-8.7640e-01$	$9.2079e-01$
$\gamma = 1.8$	U	$-6.4688e-03-3.6119e-03\mathrm{i}$	$2.6280e-01+5.3586e-01\mathrm{i}$	$1.3293e-03+8.4107e-05\mathrm{i}$
	V	$8.5856e-04+1.2580e-02\mathrm{i}$	$7.9896e-01+1.9150e-03\mathrm{i}$	$-2.3869e-03-3.0892e-03\mathrm{i}$
	Φ	$7.8123e-05$	$-9.7336e-01$	$-2.0023e-04$
	Ψ	$-9.3319e-01$	$-9.0374e-01$	$9.2079e-01$

Tables 1 and 2 exhibit the numerical solutions of $u(x,t)$, $v(x,t)$, $\phi(x,t)$ and $\psi(x,t)$ generated by the proposed schemes (19)–(30) and (125)–(134) with different γ on $[-20,20]$ at several fixed points using $h = \Delta t = \frac{1}{10}$, respectively.

The numerical errors of U^k, V^K, Φ^k and Ψ^k generated by the difference algorithm (19)–(30) with different γ are presented in Tables 3 and 4. Figures 1 and 2 display the surfaces of the

Journal Pre-proof

Table 3: Numerical results generated by the proposed scheme (19)–(30) at $T = 1$ for Example 1.

γ	h	Δt	$Err_u(h,\Delta t)$	$Err_v(h,\Delta t)$	$Err_\phi(h,\Delta t)$	$Err_\psi(h,\Delta t)$
$\gamma = 1.1$	$\frac{1}{10}$	$\frac{1}{10}$	$9.234e-03$	$1.999e-02$	$4.596e-02$	$1.737e-02$
	$\frac{1}{20}$	$\frac{1}{20}$	$2.365e-03$	$4.864e-03$	$1.245e-02$	$4.575e-03$
	$\frac{1}{40}$	$\frac{1}{40}$	$5.700e-04$	$1.155e-03$	$3.005e-03$	$1.115e-03$
	$\frac{1}{80}$	$\frac{1}{80}$	$1.145e-04$	$2.307e-04$	$6.037e-04$	$2.243e-04$
$\gamma = 1.4$	$\frac{1}{10}$	$\frac{1}{10}$	$1.000e-02$	$1.610e-02$	$4.380e-02$	$1.732e-02$
	$\frac{1}{20}$	$\frac{1}{20}$	$2.548e-03$	$3.885e-03$	$1.185e-02$	$4.560e-03$
	$\frac{1}{40}$	$\frac{1}{40}$	$6.132e-04$	$9.195e-04$	$2.867e-03$	$1.110e-03$
	$\frac{1}{80}$	$\frac{1}{80}$	$1.231e-04$	$1.837e-04$	$5.796e-04$	$2.233e-04$
$\gamma = 1.7$	$\frac{1}{10}$	$\frac{1}{10}$	$1.034e-02$	$2.386e-02$	$4.192e-02$	$1.718e-02$
	$\frac{1}{20}$	$\frac{1}{20}$	$2.640e-03$	$6.151e-03$	$1.145e-02$	$4.519e-03$
	$\frac{1}{40}$	$\frac{1}{40}$	$6.350e-04$	$1.484e-03$	$2.835e-03$	$1.098e-03$
	$\frac{1}{80}$	$\frac{1}{80}$	$1.274e-04$	$2.977e-04$	$5.731e-04$	$2.209e-04$

Table 4: Numerical results obtained by the proposed scheme (19)–(30) for Example 1.

γ	h	Δt	$Err_u(h,\Delta t)$	$Err_v(h,\Delta t)$	$Err_\phi(h,\Delta t)$	$Err_\psi(h,\Delta t)$
$\gamma = 1.3$	$\frac{1}{10}$	$\frac{1}{10}$	$9.749e-03$	$1.782e-02$	$4.459e-02$	$1.735e-02$
	$\frac{1}{20}$	$\frac{1}{20}$	$2.498e-03$	$4.287e-03$	$1.207e-02$	$4.568e-03$
	$\frac{1}{40}$	$\frac{1}{40}$	$6.012e-04$	$1.015e-03$	$2.913e-03$	$1.113e-03$
	$\frac{1}{80}$	$\frac{1}{80}$	$1.207e-04$	$2.027e-04$	$5.853e-04$	$2.238e-04$
$\gamma = 1.5$	$\frac{1}{10}$	$\frac{1}{10}$	$1.018e-02$	$1.594e-02$	$4.312e-02$	$1.728e-02$
	$\frac{1}{20}$	$\frac{1}{20}$	$2.576e-03$	$4.041e-03$	$1.160e-02$	$4.548e-03$
	$\frac{1}{40}$	$\frac{1}{40}$	$6.179e-04$	$9.689e-04$	$2.858e-03$	$1.107e-03$
	$\frac{1}{80}$	$\frac{1}{80}$	$1.239e-04$	$1.942e-04$	$5.777e-04$	$2.226e-04$
$\gamma = 1.9$	$\frac{1}{10}$	$\frac{1}{10}$	$1.242e-02$	$3.680e-02$	$4.131e-02$	$1.708e-02$
	$\frac{1}{20}$	$\frac{1}{20}$	$3.217e-03$	$9.817e-03$	$1.134e-02$	$4.496e-03$
	$\frac{1}{40}$	$\frac{1}{40}$	$7.754e-04$	$2.390e-03$	$2.808e-03$	$1.090e-03$
	$\frac{1}{80}$	$\frac{1}{80}$	$1.557e-04$	$4.808e-04$	$5.676e-04$	$2.193e-04$

discretized solutions at $T = 1$ obtained by the obtained algorithm (19)–(30) with $h = \Delta t = \frac{1}{10}$, $\gamma = 1.3$ and $\gamma = 1.8$, respectively, which further illustrates that our scheme converges to the exact solution. Figure 3 describes the RE^k with different γ, which indicates that the discrete energy conservation property is preserved. Long time computations of the RE^k with different γ is portrayed in Figure 4, which further substantiates that the suggested the obtained difference algorithm fulfills the energy preservation property. Figure 5, which is plotted on the basis of the data in Tables 3 and 4, further substantiates that the suggested scheme (19)–(30) enjoys the convergence rate of $\mathcal{O}(\Delta t^2 + h^2)$.

Journal Pre-proof

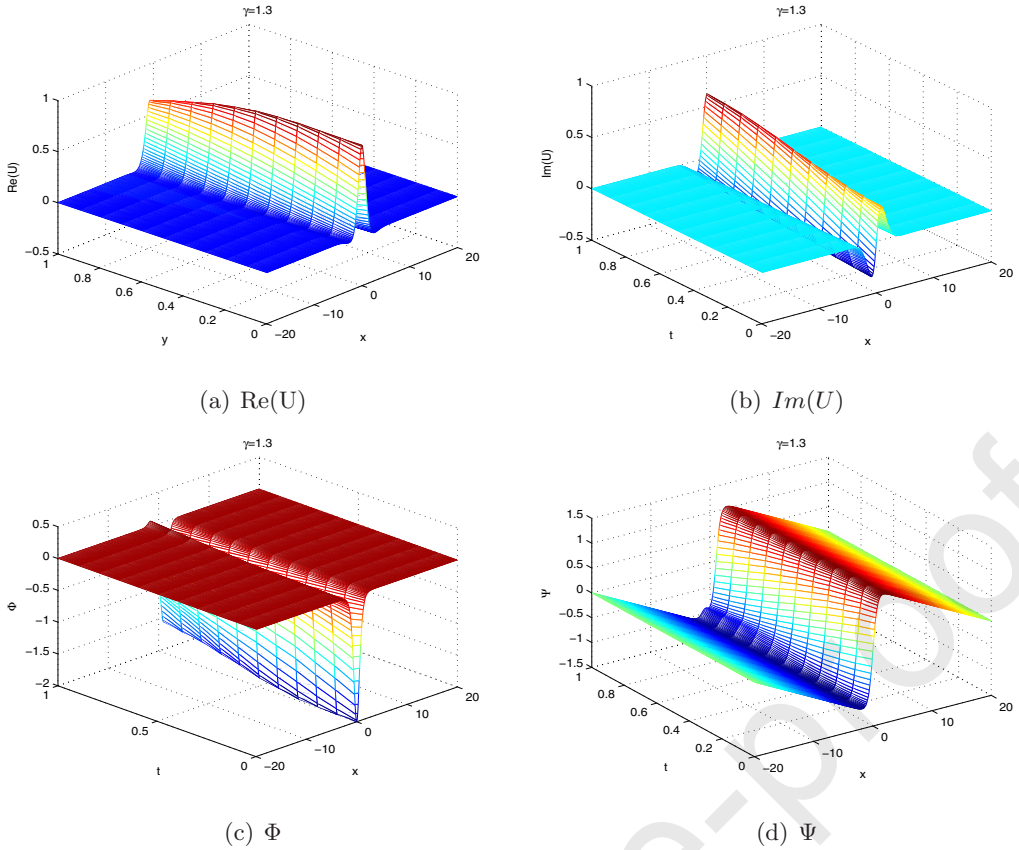

(a) Re(U) (b) $Im(U)$

(c) Φ (d) Ψ

Figure 1: The profiles of numerical solutions with $\gamma = 1.3$ achieved by the proposed scheme (19)–(30) at time $T = 1$.

The numerical errors of U^k, V^K, Φ^k and Ψ^k attained by our proposed spatial fourth-order difference algorithm (125)–(134) with different γ are listed in Tables 5 and 6. Figure 6 drawn according to the data in Tables 5 and 6 displays that as $\Delta t = h^2$, the proposed scheme (125)–(134) possesses the convergence order of $\mathcal{O}(h^4)$. Figure 7 plots the temporal convergence order of the numerical solutions got by the scheme (125)–(134). From this figure, we observe that the convergence order of the underlying scheme (125)–(134) is two in time. Figure 8 delineates the long time computations of RE^k with various γ, which substantiates that the underlying algorithm (125)–(134) satisfies the energy conservation. The errors and convergence rates of energy of schemes (19)–(30) and (125)–(134) with different γ are displayed in Tables 7, 8 and 9. From these tables, we find that the energy errors reach accuracy 10^{-13}, even 10^{-15} and are under control which further implies that the constructed schemes preserve the energy, and show a discrete consistent discretization of the underlying continuous energy conservation law. It is worthwhile to remark that the increase of relative error of energy in long time simulations might be affected by the error of the first step. Table 10 lists the absolute energy errors of scheme (19)–(30) and scheme (125)–(134) at time $t = \frac{1}{2}$, 1, 2, $\frac{7}{2}$. From this table, we observe that the suggested second-order scheme and fourth-order scheme enjoy the discrete energy conservation

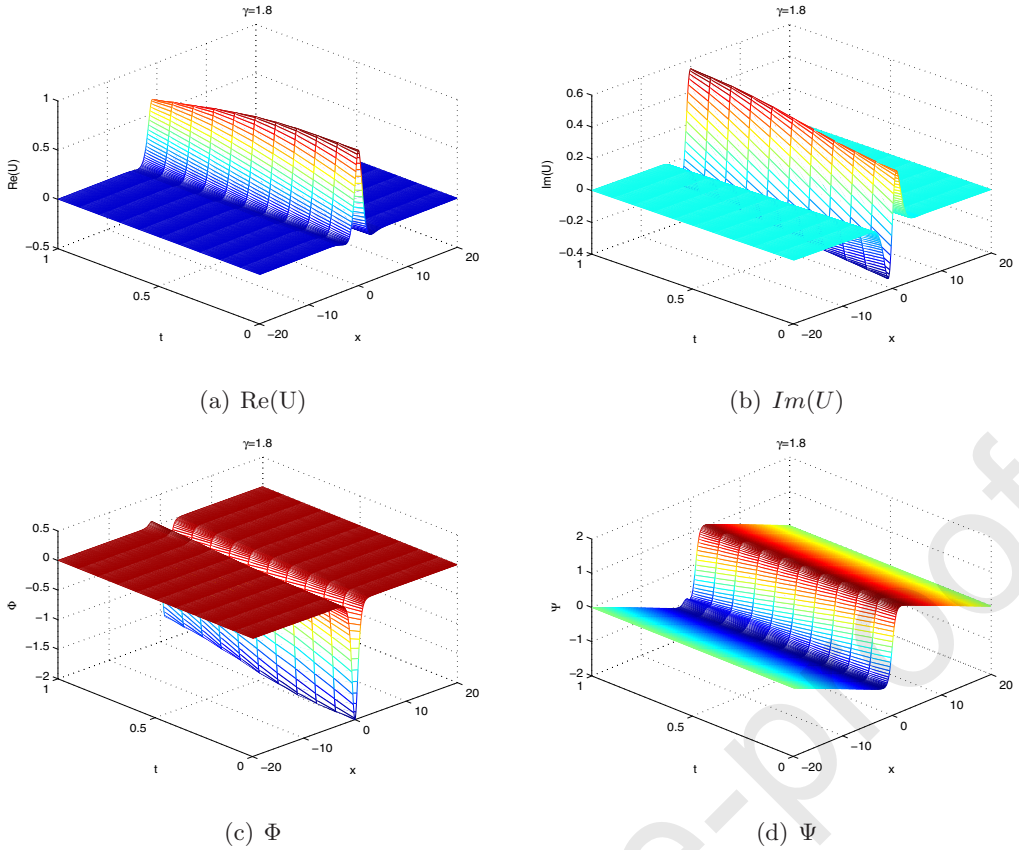

(a) Re(U) (b) $Im(U)$

(c) Φ (d) Ψ

Figure 2: The profiles of numerical solutions with $\gamma = 1.8$ generated by the proposed scheme (19)–(30) at time $T = 1$.

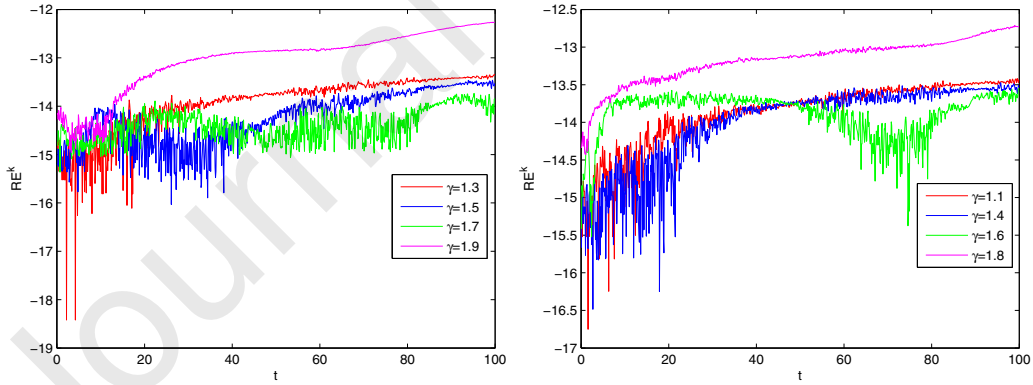

Figure 3: Example 1(obtained by the proposed scheme (19)–(30) on $[-20, 20] \times [0, 100]$ with $h = 1/10$, $\Delta t = 1/10$): Time evolution of the relative error of discrete energy RE^k with different γ.

property. And above all, the satisfaction of the discrete energy conservation law does not depend on the local truncation errors of the associated schemes. The absolute energy errors attained by

Journal Pre-proof

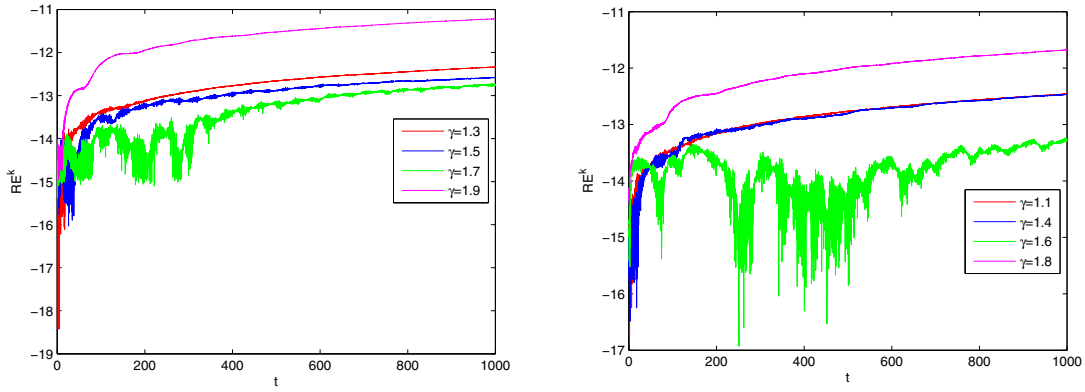

Figure 4: Example 1(derived by the proposed scheme (19)–(30) on $[-20, 20] \times [0, 1000]$ with $h = 1/10$, $\Delta t = 1/10$): Long time evolution of the relative error of discrete energy RE^k with various γ.

Table 5: Numerical results generated by the proposed scheme (125)–(134) at $T = 1$ for Example 1.

γ	h	Δt	$Err_u(h, \Delta t)$	$Err_v(h, \Delta t)$	$Err_\phi(h, \Delta t)$	$Err_\psi(h, \Delta t)$
$\gamma = 1.3$	$\frac{1}{2}$	$\frac{1}{4}$	$3.735e-02$	$8.205e-02$	$1.899e-01$	$7.351e-02$
	$\frac{1}{4}$	$\frac{1}{16}$	$3.008e-03$	$5.628e-03$	$1.860e-02$	$6.881e-03$
	$\frac{1}{8}$	$\frac{1}{64}$	$1.950e-04$	$3.615e-04$	$1.219e-03$	$4.432e-04$
	$\frac{1}{16}$	$\frac{1}{256}$	$1.164e-05$	$2.130e-05$	$7.172e-05$	$2.614e-05$
$\gamma = 1.6$	$\frac{1}{2}$	$\frac{1}{4}$	$4.760e-02$	$9.197e-02$	$1.827e-01$	$7.310e-02$
	$\frac{1}{4}$	$\frac{1}{16}$	$3.425e-03$	$7.218e-03$	$1.719e-02$	$6.808e-03$
	$\frac{1}{8}$	$\frac{1}{64}$	$2.200e-04$	$4.561e-04$	$1.173e-03$	$4.381e-04$
	$\frac{1}{16}$	$\frac{1}{256}$	$1.300e-05$	$2.688e-05$	$7.035e-05$	$2.582e-05$
$\gamma = 1.9$	$\frac{1}{2}$	$\frac{1}{4}$	$5.931e-02$	$1.620e-01$	$1.778e-01$	$7.236e-02$
	$\frac{1}{4}$	$\frac{1}{16}$	$5.116e-03$	$1.583e-02$	$1.654e-02$	$6.722e-03$
	$\frac{1}{8}$	$\frac{1}{64}$	$3.299e-04$	$1.053e-03$	$1.149e-03$	$4.326e-04$
	$\frac{1}{16}$	$\frac{1}{256}$	$1.964e-05$	$6.310e-05$	$6.911e-05$	$2.550e-05$

the proposed schemes for Example 1 on $[-20, 20] \times [0, 1]$ using different mesh size and various γ are listed in Table 11. From this table, we observe that the proposed schemes can preserve the discrete energy conservation property well. Also, the obtained discrete energy conservative property of both schemes does not depend on the the truncation errors of the proposed schemes and mesh refinements. Table 12 shows the comparison of errors of solution U^N generated by the presented schemes and other explicit scheme in [43] and the nonlinear scheme in [42] with $\gamma = 2$ for Example 1 at $T = 5$, from which we can draw that the scheme (125)–(134) produces more accurate numerical solution than scheme (19)–(30), other schemes in [43] and in [42] with the same temporal and spatial mesh-sizes. And also, with more mesh refinement, it is clear that the

Journal Pre-proof

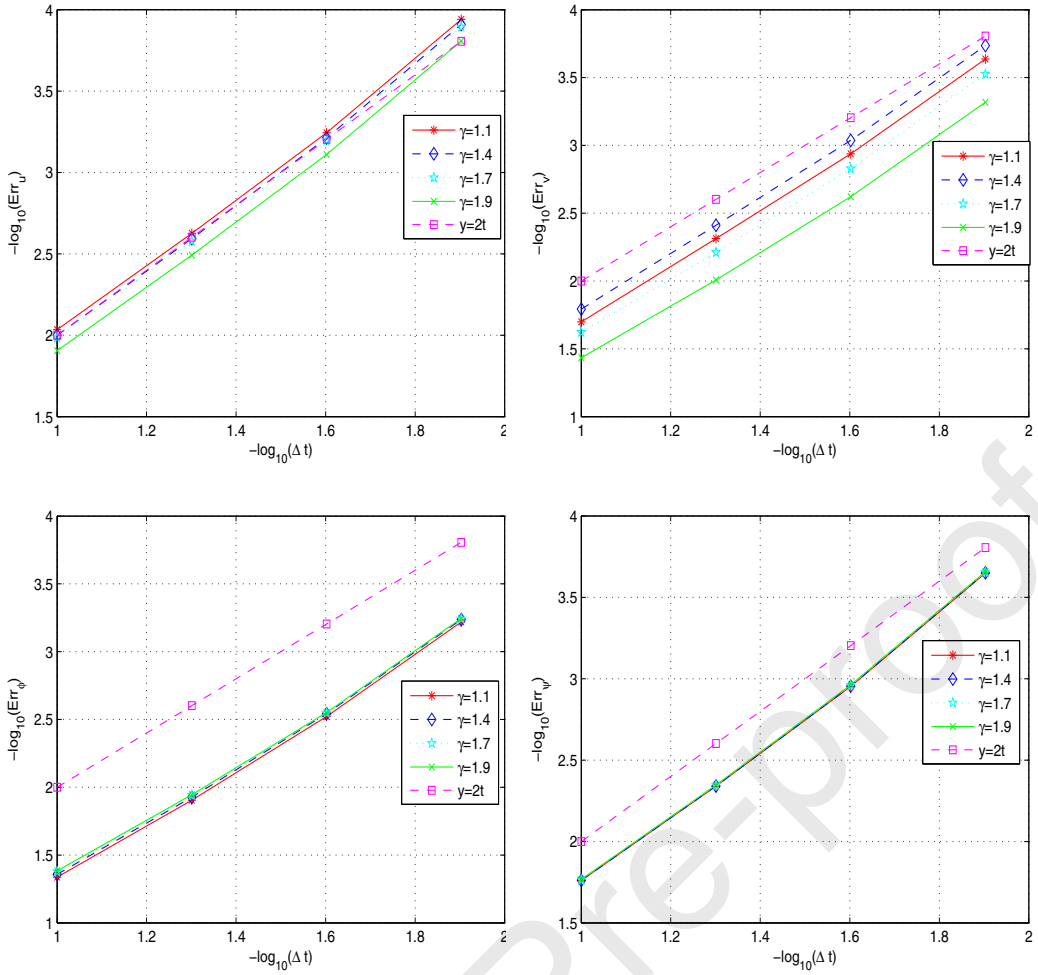

Figure 5: Convergence orders of numerical solutions at $T = 1$ for Example 1 ($\Delta t = h$).

scheme (125)–(134) outperforms other numerical schemes in term of accuracy. As for the solutions V^N, Φ^N and Ψ^N have similar numerical results. Here we omit them avoid lengthy. Besides, our schemes are unconditionally convergent and stable while the scheme in [43] is conditionally convergent and stable.

Example 2 In this example, we shall study the dynamics of wave interaction. The associated initial conditions of fractional KGZ system are taken as follows [7]:

$$\begin{aligned}
&u_0(x) = u(x - x_1, 0, \mu_1, \vartheta_1) + u(x - x_2, 0, \mu_2, \vartheta_2),\\
&u_1(x) = \tfrac{\partial u}{\partial t}(x - x_1, t, \mu_1, \vartheta_1)|_{t=0} + \tfrac{\partial u}{\partial t}(x - x_2, t, \mu_2, \vartheta_2)|_{t=0},\\
&\phi_0(x) = \phi(x - x_1, 0, \zeta_1, \vartheta_1) + \phi(x - x_2, 0, \zeta_2, \vartheta_2),\\
&\phi_1(x) = \tfrac{\partial \phi}{\partial t}(x - x_1, t, \zeta_1, \vartheta_1)|_{t=0} + \tfrac{\partial \phi}{\partial t}(x - x_2, t, \zeta_2, \vartheta_2)|_{t=0}.
\end{aligned} \tag{140}$$

Here we consider the interaction of two solitons with identical amplitudes and opposite velocities, and take $x_1 = -8$, $x_2 = 8$, $\mu_1 = \mu_2 = (\sqrt{10} - \sqrt{2})/2$, $\vartheta_1 = -\vartheta_2 = \sqrt{(\sqrt{5} - 1)/2}$. The errors and convergence order generated by the proposed scheme (125)–(134) on $[-30, 30] \times [0, 1]$ with

Journal Pre-proof

Table 6: Numerical results generated by the proposed scheme (125)–(134) at $T = 1$ for Example 1.

γ	h	Δt	$Err_u(h, \Delta t)$	$Err_v(h, \Delta t)$	$Err_\phi(h, \Delta t)$	$Err_\psi(h, \Delta t)$
$\gamma = 1.2$	$\frac{1}{2}$	$\frac{1}{4}$	$3.351e-02$	$8.227e-02$	$1.922e-01$	$7.353e-02$
	$\frac{1}{4}$	$\frac{1}{16}$	$2.756e-03$	$6.027e-03$	$1.895e-02$	$6.893e-03$
	$\frac{1}{8}$	$\frac{1}{64}$	$1.860e-04$	$3.759e-04$	$1.242e-03$	$4.440e-04$
	$\frac{1}{16}$	$\frac{1}{256}$	$1.115e-05$	$2.228e-05$	$7.310e-05$	$2.621e-05$
$\gamma = 1.5$	$\frac{1}{2}$	$\frac{1}{4}$	$4.466e-02$	$7.781e-02$	$1.850e-01$	$7.329e-02$
	$\frac{1}{4}$	$\frac{1}{16}$	$3.375e-03$	$5.741e-03$	$1.773e-02$	$6.838e-03$
	$\frac{1}{8}$	$\frac{1}{64}$	$2.132e-04$	$3.587e-04$	$1.179e-03$	$4.402e-04$
	$\frac{1}{16}$	$\frac{1}{256}$	$1.258e-05$	$2.127e-05$	$7.069e-05$	$2.594e-05$
$\gamma = 1.8$	$\frac{1}{2}$	$\frac{1}{4}$	$5.449e-02$	$1.335e-01$	$1.790e-01$	$7.261e-02$
	$\frac{1}{4}$	$\frac{1}{16}$	$4.485e-03$	$1.214e-02$	$1.656e-02$	$6.745e-03$
	$\frac{1}{8}$	$\frac{1}{64}$	$2.896e-04$	$7.951e-04$	$1.158e-03$	$4.338e-04$
	$\frac{1}{16}$	$\frac{1}{256}$	$1.713e-05$	$4.709e-05$	$6.952e-05$	$2.557e-05$

different γ for Example 2 are displayed in Tables 13 and 14, from which we observe that the convergence order of scheme (125)–(134) is two in time and four in space, respectively. Figures 9–12 got by the suggested algorithm (19)–(30) exhibit the collision course of two symmetric waves at different times with various γ. From these figures, we observe that the two waves march in the opposite directions and interact at $t = 5$. Besides, during the movement of two solitons, the soliton-like waves appear which are regularly spread. For wave forms of U^k, V^K, Φ^k and Ψ^k, one can see that the parameter γ will impact the forms of the wave. As γ decreases, the profile of the wave alters more fast, and emerge some ripples. Figure 13 derived by the suggested scheme (19)–(30) portrays the time movement of E^k and RE^k with different γ achieved by our underlying algorithm at $T = 100$. Similar numerical results derived by the suggested difference algorithm (125)–(134) are not presented here avoid lengthy.

6 Conclusions

In this paper, we developed the second-order and fourth-order linear implicit finite difference schemes with energy conservation property for solving the space fractional KGZ system (1)–(3). The energy conservation and error estimations of the suggested schemes are provided. By using discrete energy methods, we establish the optimal error estimates of the proposed schemes, without any restriction on the grid ratio. Numerical examples are performed to simulate the dynamics of wave interaction and substantiate the theoretical analysis. Lastly, we would like to point out that there are few high-order and efficient conservative numerical schemes for solving the space fractional Klein-Gordon-Zakharov system. Based on this, the proposed schemes in this paper could be an interesting contribution to the computation of fractional Klein-Gordon-

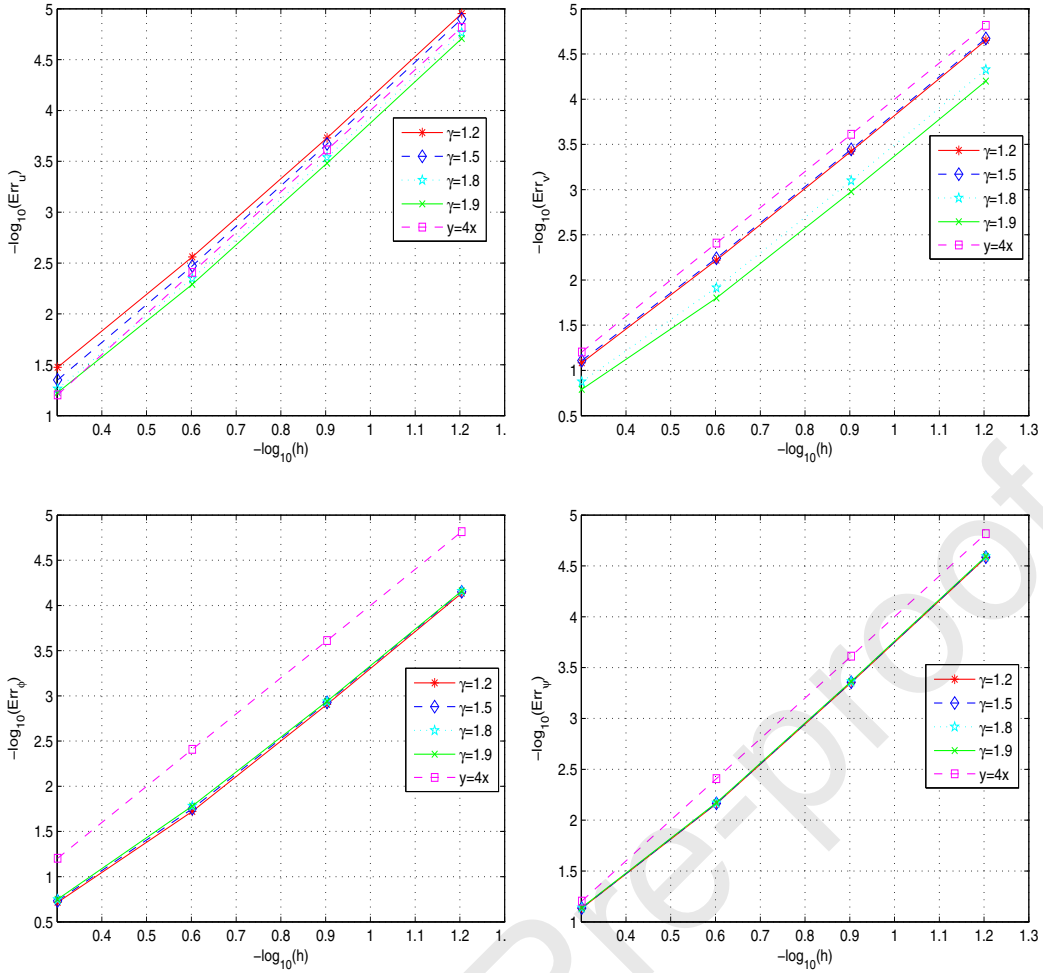

Figure 6: Spatial convergence orders of numerical solutions obtained by the scheme (125)–(134) at $T = 1$ for Example 1 ($\Delta t = h^2$).

Zakharov system. And it is also expected to provide new idea for simulating the propagation of fractional Klein-Gordon-Zakharov system accurately in fields of plasma physics, hydrodynamics and molecular dynamics. In the future, we shall continue to report the efficient numerical schemes for solving fractional Klein-Gordon-Zakharov system.

Acknowledgements

The authors would like to thank three anonymous reviewers for their valuable comments, which have helped to improve the paper greatly. This work was partially supported by the the National Natural Science Foundation of China (Grant no. 11971241) and the Natural Science Research Project of Anhui Provincial University funded by the Anhui Education Department (Grant no. KJ2020A0005).

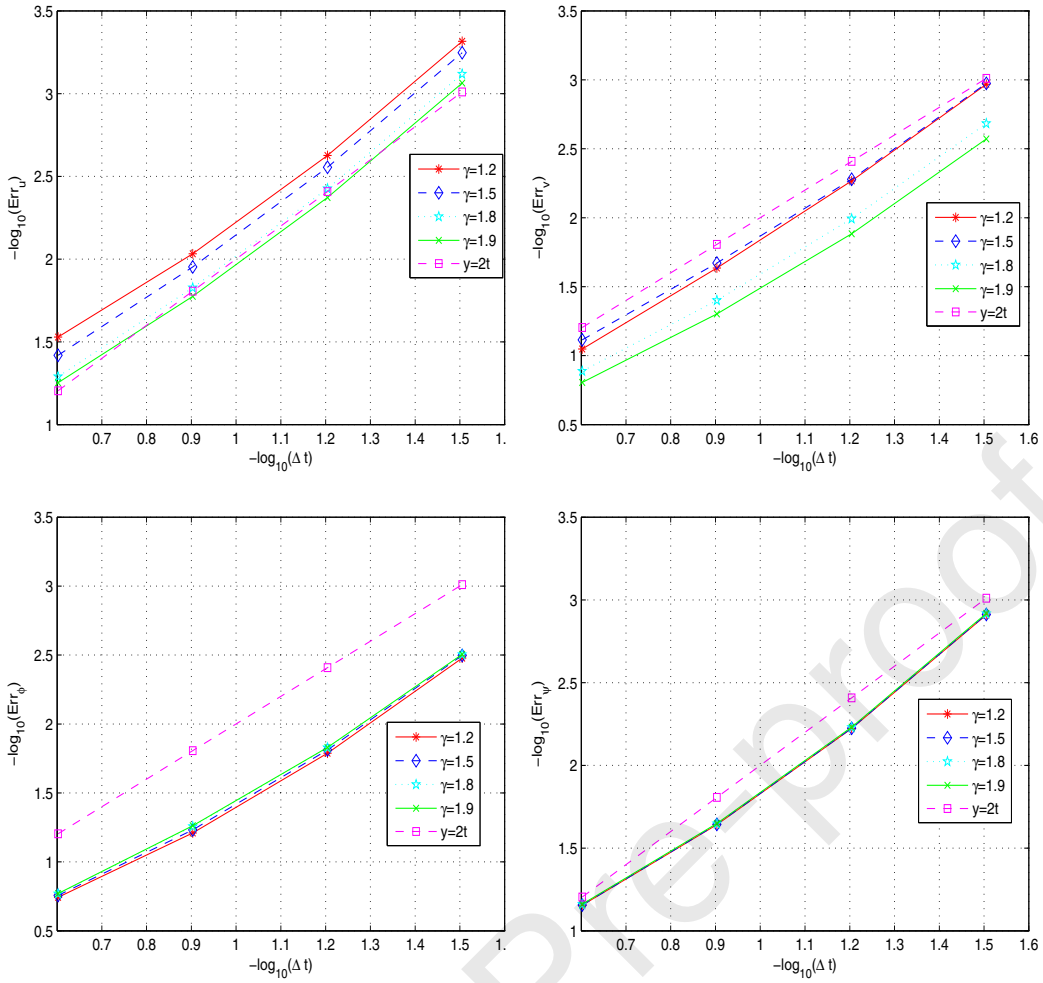

Figure 7: Temporal convergence orders of numerical solutions generated by the scheme (125)–(134) at $T = 1$ for Example 1 ($\Delta t = h$).

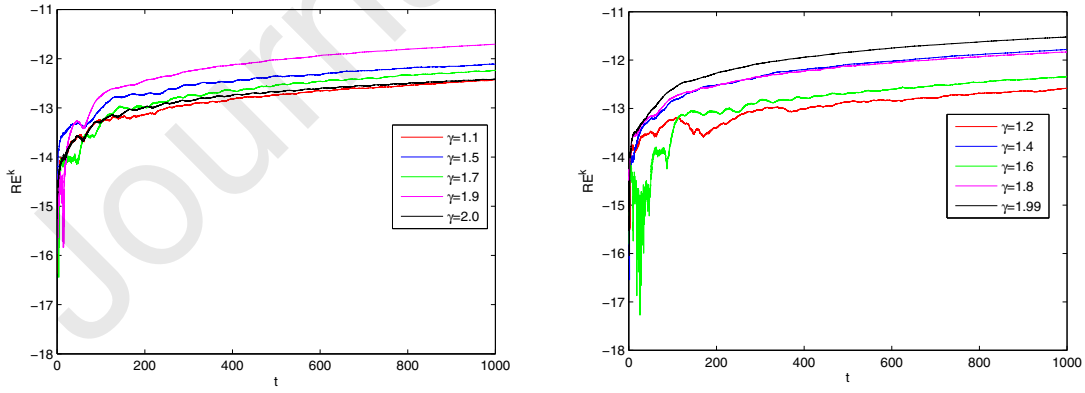

Figure 8: Example 1(derived by the proposed scheme (125)–(134) on $[-20, 20] \times [0, 1000]$ with $h = 1/4$, $\Delta t = 1/16$): Long time evolution of the relative error of discrete energy RE^k with various γ.

Journal Pre-proof

Table 7: Errors and convergence orders of energy generated by the scheme (19)–(30) for Example 1.

γ	h	Δt	Err_{energy}	$R_{energy,\Delta t}$	$R_{energy,h}$
$\gamma = 1.1$	$\frac{1}{10}$	$\frac{1}{10}$	$2.4545e-03$		
	$\frac{1}{20}$	$\frac{1}{20}$	$6.0866e-04$	2.0117	2.0117
	$\frac{1}{40}$	$\frac{1}{40}$	$1.4503e-04$	2.0693	2.0693
	$\frac{1}{80}$	$\frac{1}{80}$	$2.9012e-05$	2.3217	2.3217
$\gamma = 1.4$	$\frac{1}{10}$	$\frac{1}{10}$	$2.9452e-03$		
	$\frac{1}{20}$	$\frac{1}{20}$	$7.2964e-04$	2.0131	2.0131
	$\frac{1}{40}$	$\frac{1}{40}$	$1.7382e-04$	2.0696	2.0696
	$\frac{1}{80}$	$\frac{1}{80}$	$3.4768e-05$	2.3218	2.3218
$\gamma = 1.7$	$\frac{1}{10}$	$\frac{1}{10}$	$2.9208e-03$		
	$\frac{1}{20}$	$\frac{1}{20}$	$7.2380e-04$	2.0127	2.0127
	$\frac{1}{40}$	$\frac{1}{40}$	$1.7245e-04$	2.0694	2.0694
	$\frac{1}{80}$	$\frac{1}{80}$	$3.4495e-05$	2.3217	2.3217
$\gamma = 1.9$	$\frac{1}{10}$	$\frac{1}{10}$	$2.4084e-03$		
	$\frac{1}{20}$	$\frac{1}{20}$	$5.9882e-04$	2.0079	2.0079
	$\frac{1}{40}$	$\frac{1}{40}$	$1.4280e-04$	2.0682	2.0682
	$\frac{1}{80}$	$\frac{1}{80}$	$2.8571e-05$	2.3213	2.3213

Table 8: Errors and convergence orders of energy derived by the scheme (125)–(134) for Example 1.

γ	h	Δt	Err_{energy}	$R_{energy,\Delta t}$
$\gamma = 1.3$	$\frac{1}{2}$	$\frac{1}{2}$	$5.7614e-02$	
	$\frac{1}{4}$	$\frac{1}{4}$	$1.4724e-02$	1.9682
	$\frac{1}{8}$	$\frac{1}{8}$	$3.5561e-03$	2.0498
	$\frac{1}{16}$	$\frac{1}{16}$	$7.1507e-04$	2.3141
$\gamma = 1.5$	$\frac{1}{2}$	$\frac{1}{2}$	$5.4837e-02$	
	$\frac{1}{4}$	$\frac{1}{4}$	$1.4579e-02$	1.9113
	$\frac{1}{8}$	$\frac{1}{8}$	$3.5479e-03$	2.0388
	$\frac{1}{16}$	$\frac{1}{16}$	$7.1460e-04$	2.3118
$\gamma = 1.8$	$\frac{1}{2}$	$\frac{1}{2}$	$4.7603e-02$	
	$\frac{1}{4}$	$\frac{1}{4}$	$1.4147e-02$	1.7506
	$\frac{1}{8}$	$\frac{1}{8}$	$3.5225e-03$	2.0058
	$\frac{1}{16}$	$\frac{1}{16}$	$7.1314e-04$	2.3044
$\gamma = 1.9$	$\frac{1}{2}$	$\frac{1}{2}$	$4.4037e-02$	
	$\frac{1}{4}$	$\frac{1}{4}$	$1.3917e-02$	1.6619
	$\frac{1}{8}$	$\frac{1}{8}$	$3.5087e-03$	1.9878
	$\frac{1}{16}$	$\frac{1}{16}$	$7.1234e-04$	2.3003

Journal Pre-proof

Table 9: Errors and convergence orders of energy obtained by the scheme (125)–(134) for Example 1.

γ	h	Δt	Err_{energy}	$R_{energy,h}$
$\gamma = 1.3$	$\frac{1}{2}$	$\frac{1}{4}$	$1.1218e-02$	
	$\frac{1}{4}$	$\frac{1}{16}$	$8.1722e-04$	3.7790
	$\frac{1}{8}$	$\frac{1}{64}$	$5.0263e-05$	4.0231
	$\frac{1}{16}$	$\frac{1}{256}$	$2.9468e-06$	4.0923
$\gamma = 1.5$	$\frac{1}{2}$	$\frac{1}{4}$	$7.5048e-03$	
	$\frac{1}{4}$	$\frac{1}{16}$	$5.4598e-04$	3.7809
	$\frac{1}{8}$	$\frac{1}{64}$	$3.2808e-05$	4.0567
	$\frac{1}{16}$	$\frac{1}{256}$	$1.9119e-06$	4.1010
$\gamma = 1.8$	$\frac{1}{2}$	$\frac{1}{4}$	$1.4452e-03$	
	$\frac{1}{4}$	$\frac{1}{16}$	$1.3060e-04$	3.4680
	$\frac{1}{8}$	$\frac{1}{64}$	$1.1203e-05$	3.5433
	$\frac{1}{16}$	$\frac{1}{256}$	$7.0649e-07$	3.9870
$\gamma = 1.9$	$\frac{1}{2}$	$\frac{1}{4}$	$5.6534e-03$	
	$\frac{1}{4}$	$\frac{1}{16}$	$4.5735e-04$	3.6278
	$\frac{1}{8}$	$\frac{1}{64}$	$3.2633e-05$	3.8089
	$\frac{1}{16}$	$\frac{1}{256}$	$1.9834e-06$	4.0403

Table 10: Absolute energy errors of the proposed schemes for Example 1.

Scheme	t	$\alpha = 1.1$	$\alpha = 1.3$	$\alpha = 1.5$	$\alpha = 1.7$
Scheme (19)–(30)	$\frac{1}{2}$	$1.0663e-14$	$2.6645e-14$	$6.8989e-15$	$2.7718e-14$
	1	$7.1628e-15$	$1.6051e-14$	$5.5049e-15$	$4.2910e-14$
	2	$3.6106e-15$	$3.5775e-15$	$1.8067e-14$	$3.6061e-14$
	$\frac{7}{2}$	$1.7764e-14$	$2.0762e-15$	$2.5327e-14$	$9.8815e-15$
Scheme (125)–(134)	$\frac{1}{2}$	$2.3607e-15$	$5.4974e-15$	$4.1379e-14$	$5.5381e-14$
	1	$3.9092e-14$	$3.5799e-15$	$3.5544e-14$	$5.8977e-14$
	2	$3.1990e-14$	$1.1470e-14$	$7.7571e-14$	$8.6528e-14$
	$\frac{7}{2}$	$7.9731e-15$	$8.5428e-14$	$9.4148e-14$	$1.5029e-13$

Table 11: Absolute energy errors attained by the proposed schemes with different γ for Example 1.

Scheme	$h = \Delta t$	$\alpha = 1.4$	$\alpha = 1.6$	$\alpha = 1.8$
Scheme (19)–(30)	$\frac{1}{10}$	$8.8818e-15$	$2.8937e-14$	$4.6637e-14$
	$\frac{1}{20}$	$2.2962e-14$	$2.4907e-13$	$7.4039e-14$
Scheme (125)–(134)	$\frac{1}{10}$	$6.2212e-14$	$2.4039e-14$	$1.0170e-13$
	$\frac{1}{20}$	$1.9549e-13$	$1.5458e-13$	$4.4451e-14$

Journal Pre-proof

Table 12: The comparison of errors of solution to different numerical schemes for Example 1 at $T = 5$.

Δt	h	Scheme in [43]	Scheme in [42]	Scheme (19)–(30)	Scheme (125)–(134)
0.04	$\frac{1}{2}$	$3.126e-02$	$2.729e-02$	$8.984e-02$	$2.298e-02$
	$\frac{1}{4}$	$9.311e-03$	$8.434e-03$	$2.818e-02$	$3.232e-03$
	$\frac{1}{8}$	$2.702e-03$	$2.504e-03$	$7.145e-03$	$2.492e-04$
	$\frac{1}{16}$	$7.593e-04$	$7.452e-04$	$1.455e-03$	$1.529e-05$
0.01	$\frac{1}{2}$	$2.322e-03$	$4.270e-03$	$8.990e-02$	$2.331e-02$
	$\frac{1}{4}$	$6.303e-04$	$1.183e-03$	$2.888e-02$	$3.449e-03$
	$\frac{1}{8}$	$1.635e-04$	$3.179e-04$	$7.540e-03$	$2.800e-04$
	$\frac{1}{16}$	$4.144e-05$	$8.177e-05$	$1.540e-03$	$1.723e-05$

Table 13: Errors and temporal convergence order generated by the proposed scheme (125)–(134) at $T = 1$ for Example 2. ($h = \Delta t$)

γ	Δt	$Err_u(h,\Delta t)$	$R_{u,\Delta t}$	$Err_v(h,\Delta t)$	$R_{v,\Delta t}$	$Err_\phi(h,\Delta t)$	$R_{\phi,\Delta t}$	$Err_\psi(h,\Delta t)$	$R_{\psi,\Delta t}$
$\gamma = 1.5$	$\frac{1}{4}$	$3.8131e-02$		$7.6837e-02$		$1.7525e-01$		$6.9861e-02$	
	$\frac{1}{8}$	$1.1154e-02$	1.7733	$2.1305e-02$	1.8506	$5.8676e-02$	1.5786	$2.2742e-02$	1.6191
	$\frac{1}{16}$	$2.7867e-03$	2.0010	$5.2553e-03$	2.0194	$1.5426e-02$	1.9274	$5.9613e-03$	1.9317
	$\frac{1}{32}$	$5.6590e-04$	2.2999	$1.0597e-03$	2.3102	$3.1822e-03$	2.2773	$1.2239e-03$	2.2841
$\gamma = 1.7$	$\frac{1}{4}$	$4.6692e-02$		$1.0758e-01$		$1.7186e-01$		$6.9508e-02$	
	$\frac{1}{8}$	$1.3318e-02$	1.8098	$3.1857e-02$	1.7558	$5.6434e-02$	1.6066	$2.2598e-02$	1.6210
	$\frac{1}{16}$	$3.3165e-03$	2.0056	$7.9836e-03$	1.9965	$1.4901e-02$	1.9212	$5.9201e-03$	1.9325
	$\frac{1}{32}$	$6.7202e-04$	2.3031	$1.6207e-03$	2.3004	$3.1571e-03$	2.2387	$1.2151e-03$	2.2846
$\gamma = 1.9$	$\frac{1}{4}$	$5.5860e-02$		$1.5659e-01$		$1.6967e-01$		$6.9053e-02$	
	$\frac{1}{8}$	$1.6784e-02$	1.7348	$4.9859e-02$	1.6511	$5.4626e-02$	1.6351	$2.2444e-02$	1.6214
	$\frac{1}{16}$	$4.2450e-03$	1.9832	$1.3064e-02$	1.9322	$1.4794e-02$	1.8846	$5.8798e-03$	1.9325
	$\frac{1}{32}$	$8.6408e-04$	2.2965	$2.6855e-03$	2.2823	$3.1268e-03$	2.2422	$1.2070e-03$	2.2843

Table 14: Errors and spatial convergence order generated by the proposed scheme (125)–(134) at $T = 1$ for Example 2. ($\Delta t = h^2$)

γ	h	$Err_u(h,\Delta t)$	$R_{u,h}$	$Err_v(h,\Delta t)$	$R_{v,h}$	$Err_\phi(h,\Delta t)$	$R_{\phi,h}$	$Err_\psi(h,\Delta t)$	$R_{\psi,h}$
$\gamma = 1.5$	$\frac{1}{2}$	$4.4657e-02$		$7.7817e-02$		$1.8499e-01$		$7.3097e-02$	
	$\frac{1}{4}$	$3.3746e-03$	3.7261	$5.7409e-03$	3.7607	$1.7725e-02$	3.3836	$6.8381e-03$	3.4182
	$\frac{1}{8}$	$2.1322e-04$	3.9843	$3.5869e-04$	4.0005	$1.1792e-03$	3.9099	$4.4018e-04$	3.9574
	$\frac{1}{16}$	$1.2580e-05$	4.0831	$2.1270e-05$	4.0759	$7.0692e-05$	4.0601	$2.5941e-05$	4.0848
$\gamma = 1.7$	$\frac{1}{2}$	$4.9708e-02$		$1.1028e-01$		$1.8064e-01$		$7.2672e-02$	
	$\frac{1}{4}$	$3.9082e-03$	3.6689	$9.2974e-03$	3.5682	$1.6622e-02$	3.4419	$6.7753e-03$	3.4230
	$\frac{1}{8}$	$2.5140e-04$	3.9585	$5.9706e-04$	3.9609	$1.1662e-03$	3.8333	$4.3582e-04$	3.9585
	$\frac{1}{16}$	$1.4929e-05$	4.0738	$3.5256e-05$	4.0819	$6.9951e-05$	4.0593	$2.5684e-05$	4.0848
$\gamma = 1.9$	$\frac{1}{2}$	$5.9305e-02$		$1.6198e-01$		$1.7783e-01$		$7.2159e-02$	
	$\frac{1}{4}$	$5.1135e-03$	3.5358	$1.5830e-02$	3.3551	$1.6543e-02$	3.4262	$6.7220e-03$	3.4242
	$\frac{1}{8}$	$3.2988e-04$	3.9543	$1.0531e-03$	3.9099	$1.1490e-03$	3.8477	$4.3255e-04$	3.9579
	$\frac{1}{16}$	$1.9640e-05$	4.0701	$6.3096e-05$	4.0610	$6.9114e-05$	4.0553	$2.5496e-05$	4.0845

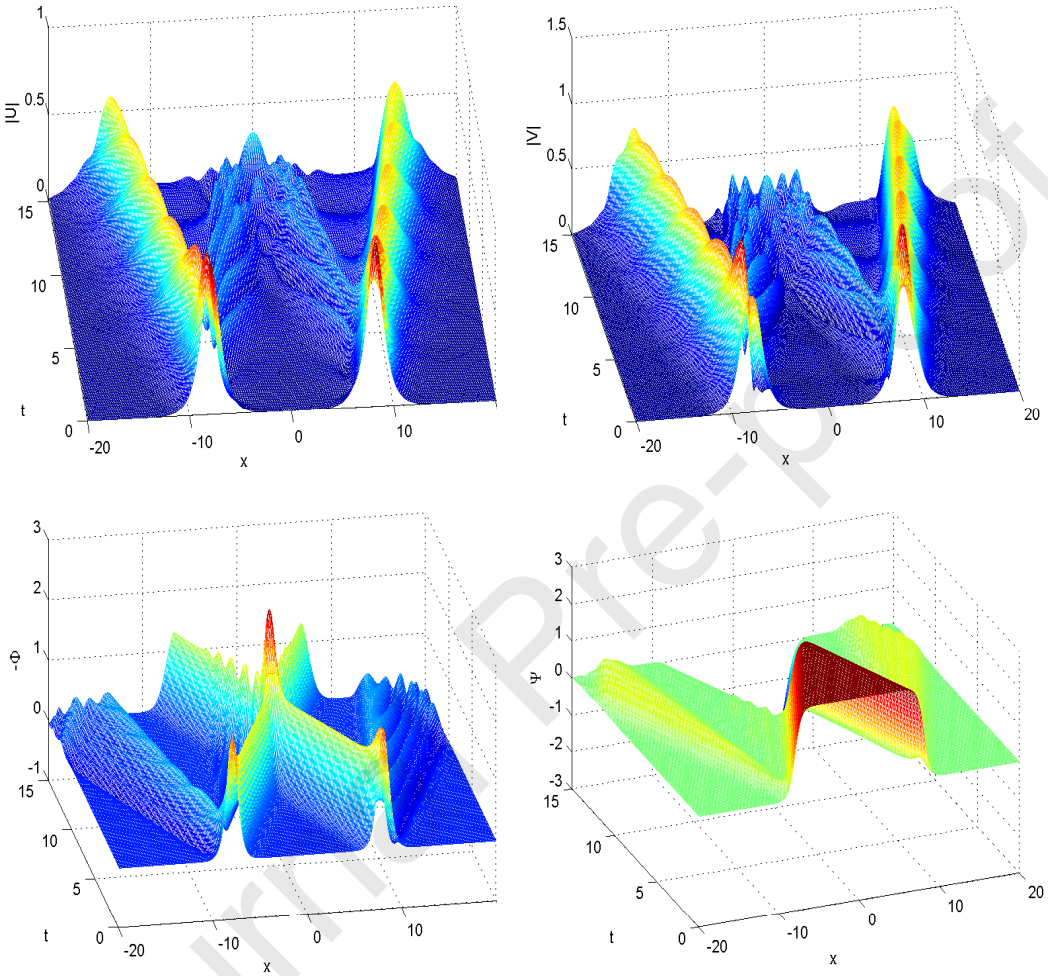

Figure 9: Example 2(obtained by the proposed scheme (19)–(30) on $[-20, 20] \times [0, 15]$ with $h = \Delta t = 1/10$):Surface plot of interaction of two solitons, $\gamma = 1.2$.

Journal Pre-proof

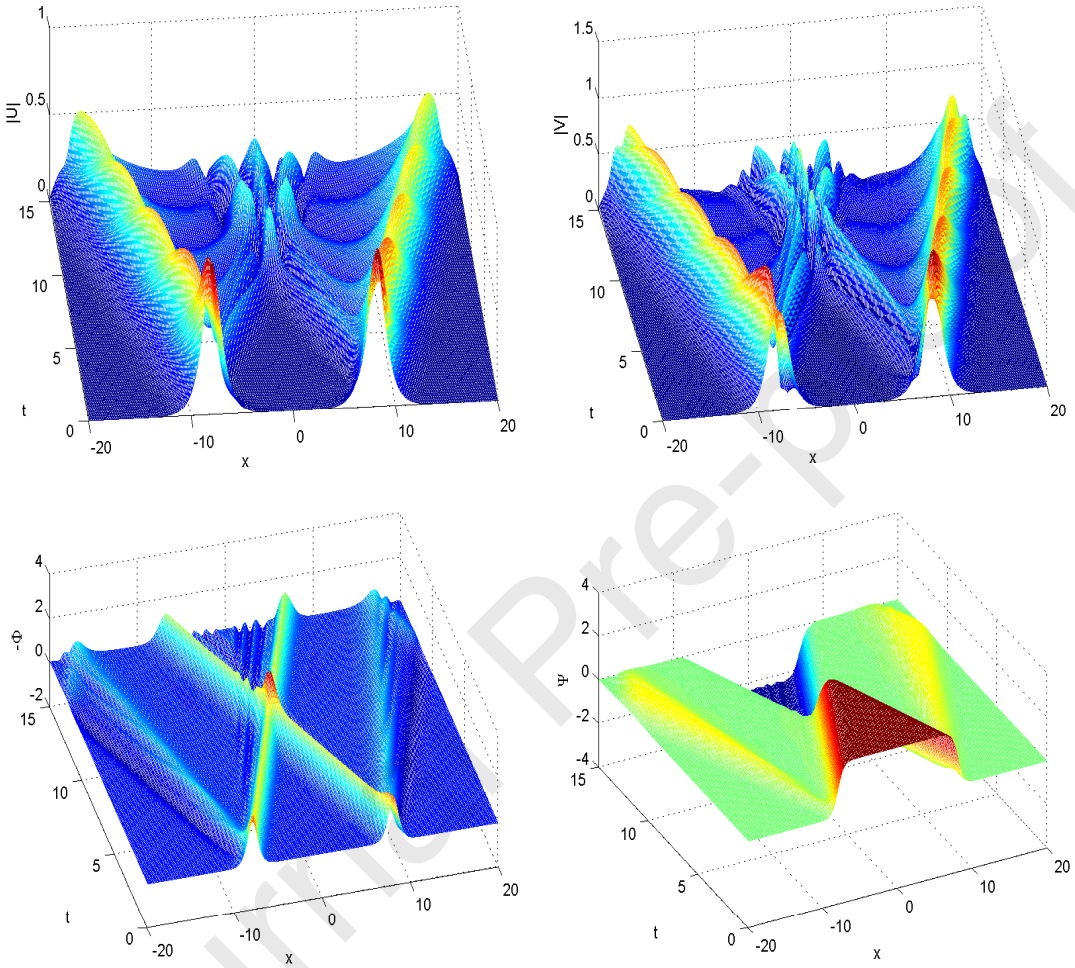

Figure 10: Example 2(derived by the proposed scheme (19)–(30) on $[-20, 20] \times [0, 15]$ with $h = \Delta t = 1/10$):Surface plot of interaction of two solitons, $\gamma = 1.7$.

Journal Pre-proof

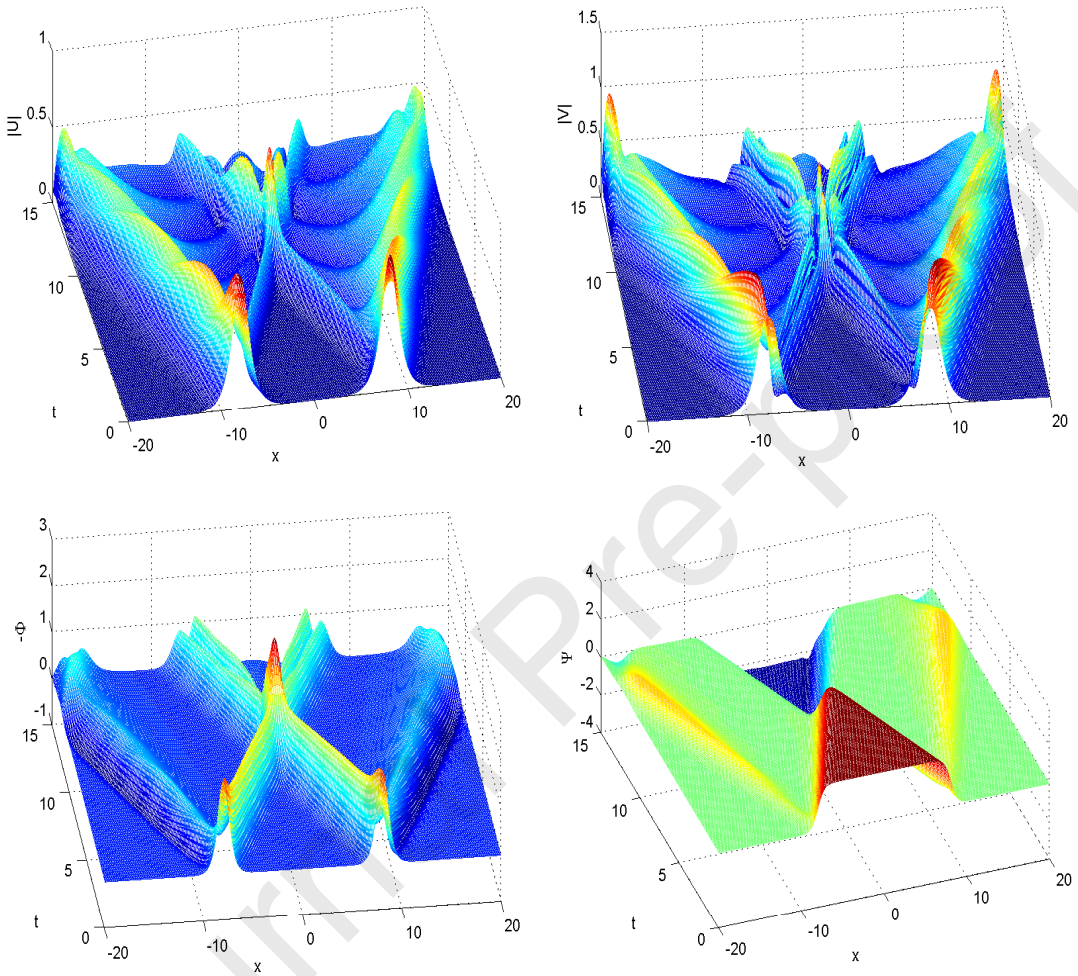

Figure 11: Example 2(obtained by the proposed scheme (19)–(30) on $[-20, 20] \times [0, 15]$ with $h = \Delta t = 1/10$):Surface plot of interaction of two solitons, $\gamma = 1.99$.

Journal Pre-proof

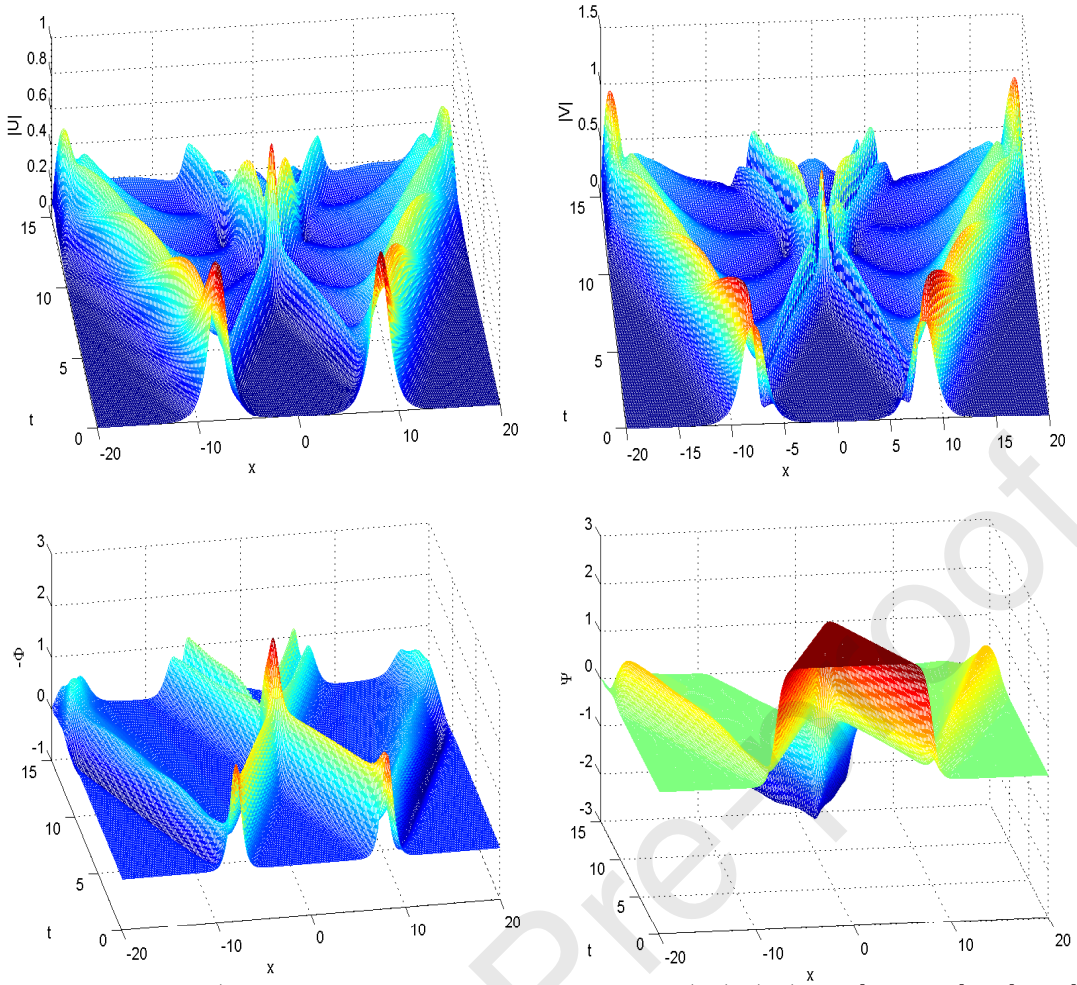

Figure 12: Example 2(generated by the proposed scheme (19)–(30) on $[-20, 20] \times [0, 15]$ with $h = \Delta t = 1/10$):Surface plot of interaction of two solitons, $\gamma = 2$.

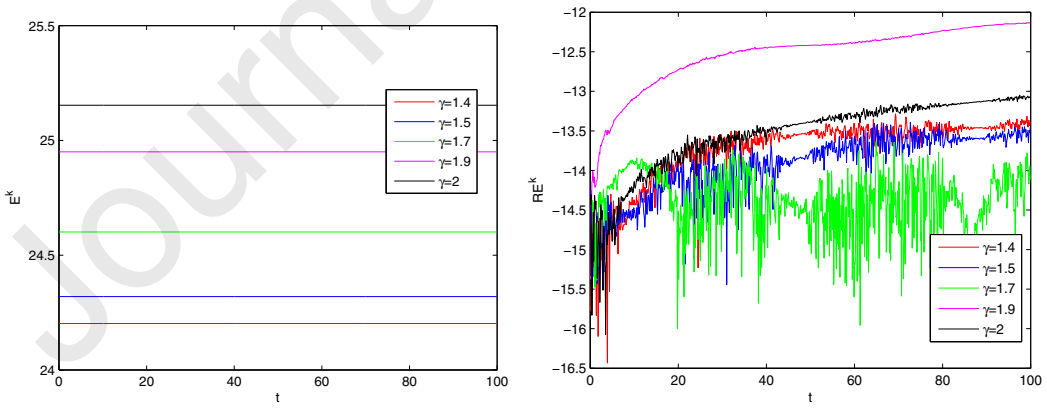

Figure 13: Example 1(obtained by our scheme (19)–(30) on $[-20, 20] \times [0, 100]$ with $h = 1/10$, $\Delta t = 1/10$): Time evolution of the discrete energy E^k (left column) and associated relative error of discrete energy RE^k (right column) with different γ.

Journal Pre-proof

References

[1] Q. Yang, F. Liu, I. Turner, Numerical methods for fractional partial differential equations with Riesz space fractional derivatives, Appl. Math. Model., 34 (2010), 200–218.

[2] I. Podlubny, Fractional Differential Equations, Academic Press, New York, 1999.

[3] M.S. Ismail, A. Biswas, 1-Soliton solution of the Klein-Gordon-Zakharov equation with power law nonlinearity, Appl. Math. Comput., 217 (2010), 4186–4196.

[4] T. Wang, J. Chen, L. Zhang, Conservative difference methods for the Klein-Gordon-Zakharov equations, J. Comput. Appl. Math., 205 (2007), 430–452.

[5] W. Bao, X. Dong, X. Zhao, An exponential wave integrator pseudospectral method for the Klein-Gordon-Zakharov system, SIAM J. Sci. Comput., 35 (2013), 2903–2927.

[6] W. Bao, C. Su, Uniform error bounds of a finite difference method for the Klein-Gordon-Zakharov system in the subsonic limit regime, Math. Comput., 87 (2018), 2133–2158.

[7] M. Dehghan, A. Nikpour, The solitary wave solution of coupled Klein-Gordon-Zakharov equations via two different numerical methods, Comput. Phys. Commun., 184 (2013), 2145–2158.

[8] M. Dehghan, M. Abbaszadeh, Solution of multi-dimensional Klein-Gordon-Zakharov and Schrödinger/Gross-Pitaevskii equations via local Radial Basis Functions-Differential Quadrature (RBF-DQ) technique on non-rectangular computational domains, Eng. Anal. Bound. Elem., 92 (2018), 156–170.

[9] M. Dehghan, A. Taleei, Numerical solution of the Yukawa-coupled Klein-Gordon-Schrödinger equations via a Chebyshev pseudospectral multidomain method, Appl. Math. Model., 36 (2012), 2340–2349.

[10] M. Dehghan, Finite difference procedures for solving a problem arising in modeling and design of certain optoelectronic devices, Math. Comput. Simulat., 71 (2006), 16–30.

[11] J. Xie, Z. Zhang, An analysis of implicit conservative difference solver for fractional Klein-Gordon-Zakharov system, Appl. Math. Comput., 348 (2019), 153–166.

[12] B. Guo, Y. Han, J. Xin, Existence of the global smooth solution to the period boundary value problem of fractional nonlinear Schrödinger equation, Appl. Math. Comput., 204 (2008), 468–477.

[13] W. Chen, X. Li, D. Liang, Energy-conserved splitting FDTD methods for Maxwell's equations, Numer. Math., 108 (2008), 445–485.

[14] L. Brugnano, F. Iavernaro, Line integral methods for conservative problems, CRC Press, Boca Raton, FL, 2016.

Journal Pre-proof

[15] Q. Wang, Z. Zhang, X. Zhang, Q. Zhu, Energy-preserving finite volume element method for the improved Boussinesq equation, J. Comput. Phys., 270 (2014), 58–69.

[16] M. Dahlby, B. Owren, A general framework for deriving integral preserving numerical methods for PDEs, SIAM J. Sci. Comput., 33 (2011), 2318–2340.

[17] S. Eidnes, L. Li, S. Sato, Linearly implicit structure-preserving schemes for Hamiltonian systems, J. Comput. Appl. Math., 387 (2021), 112489.

[18] J. Xie, Z. Zhang, Efficient linear energy dissipative difference schemes for the coupled nonlinear damped space fractional wave equations, Commun. Nonlinear Sci. Numer. Simulat., 90 (2020), 105291.

[19] Z. Qiao, Z. Zhang, T. Tang, An adaptive time-stepping strategy for the molecular beam epitaxy models, SIAM J. Sci. Comput., 33 (2011), 1395–1414.

[20] K. Wu, H. Tang, High-order accurate physical-constraints-preserving finite difference WENO schemes for special relativistic hydrodynamics, J. Comput. Phys., 298 (2015), 539–564.

[21] R. Abgrall, D. Torlo, High order asymptotic preserving deferred correction implicit-explicit schemes for kinetic models, SIAM J. Sci. Comput., 42 (2020), 816–845.

[22] Q. Du, L. Ju, X. Li, Z. Qiao, Maximum principle preserving exponential time differencing schemes for the nonlocal Allen-Cahn equation, SIAM J. Numer. Anal., 57 (2019), 875–898.

[23] J. Shen, T. Tang, J. Yang, On the maximum principle preserving schemes for the generalized Allen-Cahn equation, Commun. Math. Sci., 14 (2016), 1517–1534.

[24] Y. Gong, J. Zhao, X. Yang, Q. Wang, Fully discrete second-order linear schemes for hydrodynamic phase field models of binary viscous fluid flows with variable densities, SIAM J. Sci. Comput., 40 (2018), 138–167.

[25] A. Mohebbi, M. Abbaszadeh, M. Dehghan, The use of a meshless technique based on collocation and radial basis functions for solving the time fractional nonlinear Schrödinger equation arising in quantum mechanics, Eng. Anal. Bound. Elem., 37 (2013), 475–485.

[26] M. Dehghan, J. Manafian, A. Saadatmandi, Solving nonlinear fractional partial differential equations using the homotopy analysis method, Numer. Methods Partial Diff. Eqns., 26 (2010), 448–479.

[27] T. Arakawa, T. Ibukiyama, M. Kaneko, Bernoulli Numbers and Zeta Functions, Springer, Japan, 2014.

[28] D.E. Knuth, T.J. Buckholtz, Computation of Tangent, Euler, and Bernoulli numbers, Math. Comp., 21 (1967), 663–688.

Journal Pre-proof

[29] P. Rahimkhani, Y. Ordokhani, E. Babolian, Fractional-order Bernoulli functions and their applications in solving fractional Fredholem-Volterra integro-differential equations, Appl. Numer. Math., 122 (2017), 66–81.

[30] X. Zhao, Z. Sun, Z. Hao, A fourth-order compact ADI scheme for two-dimensional nonlinear space fractional Schrodinger equation, SIAM J. Sci. Comput., 36 (2014), 2865–2886.

[31] W. Tian, H. Zhou, W. Deng, A class of second order difference approximation for solving space fractional diffusion equations, Math. Comp., 84 (2015), 1703–1727.

[32] Z. Yang, Z. Yuan, Y. Nie, J. Wang, X. Zhu, F. Liu, Finite element method for nonlinear Riesz space fractional diffusion equations on irregular domains, J. Comput. Phys., 330 (2017), 863–883.

[33] N. Du, H. Wang, A fast finite element method for space-fractional dispersion equations on bounded domains in R^2, SIAM J. Sci. Comput., 37 (2015), 1614–1635.

[34] B. Jin, R. Lazarov, J. Pasciak, W. Rundell, Variational formulation of problems involving fractional order differential operators, Math. Comp., 84 (2015), 2665–2700.

[35] H. Fu, H. Liu, H. Wang, A finite volume method for two-dimensional Riemann-Liouville space-fractional diffusion equation and its efficient implementation, J. Comput. Phys., 388 (2019), 316–334.

[36] H. Zhang, X. Jiang, F. Zeng, G. Karniadakis, A stabilized semi-implicit Fourier spectral method for nonlinear space-fractional reaction-diffusion equations, J. Comput. Phys., 405 (2020), 109141.

[37] F. Zeng, F. Liu, C. Li, K. Burrage, I. Turner, V. Anh, A Crank-Nicolson ADI spectral method for the two-dimensional Riesz space fractional nonlinear reaction-diffusion equation, SIAM J. Numer. Anal., 52 (2014), 2599–2622.

[38] P. Wang, C. Huang, L. Zhao, Point-wise error estimate of a conservative difference scheme for the fractional Schrödinger equation, J. Comput. Appl. Math., 306 (2016), 231–247.

[39] M. Ran, C. Zhang, A conservative difference scheme for solving the strongly coupled nonlinear fractional Schrödinger equations, Commun. Nonlinear Sci. Numer. Simulat., 41 (2016), 64–83.

[40] M. Li, X. Gu, C. Huang, M. Fei, G. Zhang, A fast linearized conservative finite element method for the strongly coupled nonlinear fractional Schrödinger equations, J. Comput. Phys., 358 (2018), 256–282.

[41] A. Xiao, J. Wang, Symplectic scheme for the Schrödinger equation with fractional Laplacian, Appl. Numer. Math., 146 (2019), 469–487.

Journal Pre-proof

[42] A. Hendy, J.E. Macías-Díaz, A numerically efficient and conservative model for a Riesz space-fractional Klein-Gordon-Zakharov system, Commun. Nonlinear Sci. Numer. Simulat., 71 (2019), 22–37.

[43] R. Martínez, J.E. Macías-Díaz, A.S. Hendy, Theoretical analysis of an explicit energy-conserving scheme for a fractional Klein-Gordon-Zakharov system, Appl. Numer. Math., 146 (2019), 245–259.

[44] J.E. Macías-Díaz, A structure-preserving method for a class of nonlinear dissipative wave equations with Riesz space-fractional derivatives, J. Comput. Phys., 351 (2017), 40–58.

[45] Y. Fu, W. Cai, Y. Wang, An explicit structure-preserving algorithm for the nonlinear fractional Hamiltonian wave equation, Appl. Math. Lett., 102 (2020), 106123.

[46] B. Hou, D. Liang, Time fourth-order energy-preserving AVF finite difference method for nonlinear space-fractional wave equations, J. Comput. Appl. Math., 386 (2021), 113227.

[47] J. Xie, Z. Zhang, D. Liang, A conservative splitting difference scheme for the fractional-in-space Boussinesq equation, Appl. Numer. Math., 143 (2019), 61–74.

[48] J. Xie, D. Liang, Z. Zhang, Two novel energy dissipative difference schemes for the strongly coupled nonlinear space fractional wave equations with damping, Appl. Numer. Math., 157 (2020), 178–209.

[49] J. Xie, Z. Zhang, D. Liang, A new fourth-order energy dissipative difference method for high-dimensional nonlinear fractional generalized wave equations, Commun. Nonlinear Sci. Numer. Simulat., 78 (2019), 104850.

[50] Z. Hao, Z. Sun, W. Cao, A fourth-order approximation of fractional derivatives with its applications, J. Comput. Phys., 281 (2015), 787–805.

[51] Z. Sun, Numerical Methods for Partial Differential Equations, second ed., Science Press, Beijing, 2012. (In Chinese).

[52] W. Bao, Y. Cai, Optimal error estimates of finite difference methods for the Gross-Pitaevskii equation with angular momentum rotation, Math. Comp., 82 (2013), 99–128.

[53] D. Deng, C. Zhang, Analysis and application of a compact multistep ADI solver for a class of nonlinear viscous wave equations, Appl. Math. Model., 39 (2015), 1033–1049.

[54] D. Deng, D. Liang, The energy preserving finite difference methods and their analyses for system of nonlinear wave equations in two dimensions, Appl. Numer. Math., 151 (2020), 172–198.